The Pennsylvania State University

The Graduate School

Mechanical Engineering Department

NON-INTRUSIVE DRIVER DROWSINESS MONITORING VIA ARTIFICIAL NEURAL NETWORKS

A Thesis in

Mechanical Engineering

by

Jonathan Culp

Submitted in Partial Fulfillment
of the Requirements
for the Degree of

Master of Science

May 2008

The thesis of Jonathan Culp was reviewed and approved* by the following:

Moustafa El-Gindy
Senior Scientist, Applied Research Laboratory
Thesis Co-Advisor

M. Aman Haque
Assistant Professor of Mechanical Engineering
Thesis Co-Advisor

Sean Brennan
Assistant Professor of Mechanical Engineering

Karen A. Thole
Professor of Mechanical Engineering
Department Head of Mechanical and Nuclear Engineering

*Signatures are on file in the Graduate School

ABSTRACT

A completely non-intrusive method of monitoring driver drowsiness is described. Because of their abilities to learn behavior and represent very complex relationships, artificial neural networks are the basis of the method presented. Four artificial neural networks are designed based on the hypothesis that the time derivative of force (jerk) exerted by the driver at the steering wheel and accelerator pedal can be used to discern levels of alertness. The artificial neural networks are trained to replicate non-drowsy input, and then tested with unseen data. Data sets that are similar to the training sets will pass through the network with little change, and sets that are different will be changed considerably by the network. Thus, the further the driver's jerk profile deviates from the non-drowsy jerk profile, the greater the error between the input and output of the network will be. The changes in network error with drive time are presented from testing the networks with simulated driving data, and the performance of the artificial neural network designs are compared.

TABLE OF CONTENTS

LIST OF FIGURES vi

LIST OF TABLES viii

ACKNOWLEDGEMENTS ix

CHAPTER 1: LITERATURE REVIEW OF DRIVER ALERTNESS MONITORING TECHNIQUES 1

Introduction 1

Causes of Alertness Impairment 2

Human Sleepiness 2

Fatigue 4

Monotony 6

Driver Alertness Monitoring Techniques 6

Car Observation Systems 7

Driver Observation Systems 8

Car-Driver Interface Observation Systems 12

Alertness Prediction Using Artificial Neural Networks 16

Literature Review Conclusions 25

CHAPTER 2: DRIVER ALERTNESS EXPERIMENT AT THE PENN STATE TRUCK DRIVING SIMULATOR 27

Overview of Simulator Architecture 27

Driving Scenario Development 30

Experimental Procedures 35

Data Recording 36

CHAPTER 3: ARTIFICIAL NEURAL NETWORKS ARCHITECTURE AND TRAINING 37

Introduction 37

Artificial Neural Network Training with Back Propagation 41

Alternative *Networks* 44

CHAPTER 4: APPROACH 47

System Overview 47

Input Processing 49

Savitzky-Golay Filter for Numerical Differentiation 49

Spikiness Index 53

Artificial Neural Network Designs 55

Network Training 56

CHAPTER 5: RESULTS 60

Jerk Profile 60

Spikiness Index 65

Chapter 6: Conclusion 71

References 73

LIST OF FIGURES

Figure 1.1: Factors Contributing to Vehicle Driver Fatigue (Dawson et al., 2001) 5

Figure 1.2: Linear and Parabolic Regimens (Jung and Kelber, 2005)..... 8

Figure 1.3: Flow Chart for Vision/Context-Based System (Ji, et al., 2004) 10

Figure 1.4: Graphical Representation of Spikiness Index (Haque and Desai, 2006) 14

Figure 1.5: Flow Chart for AWAKE System (Bekiaris et al. 2004)..... 15

Figure 1.6: Flow chart for EEG Analysis System (Wilson and Bracewell, 2000)..... 19

Figure 1.7: Spring-Damper Representation of Human Body (Andreeya, 2004)..... 20

Figure 1.8: Biological and Driving Signal System (Hayashi et al., 2000)..... 23

Figure 1.9: Normal and Abnormal Trajectories (Carswell and Chandran, 1994)..... 24

Figure 2.1: The Pennsylvania State Truck Driving Simulator 28

Figure 2.3: Map of “Mountain” Terrain Used for Driving Scenario..... 32

Figure 2.4: Simulated Vehicle Setup..... 33

Figure 2.5: Mice Window Showing Data Recording Tasks..... 34

Figure 3.1:Diagram of Neuron 37

Figure 3.2: Diagram of a Three-Layer Feed-forward ANN 38

Figure 3.3: MATLAB Hard Limit Function 40

Figure 3.4: MATLAB Log-Sigmoid Function 41

Figure 3.5: MATLAB Radial Basis Function..... 45

Figure 3.6: Radial Basis Neuron 46

Figure 4.1: System Flow Chart 48

Figure 4.2: Raw and Smoothed Steering Position Data 52

Figure 4.3: Raw and Smoothed Accelerator Pedal Position Data 53

Figure 4.4: Definition of Spikiness (Desai and Haque, 2006)..... 54

Figure 4.5: Example Training Record for Feedforward Network Using Jerk Profile..... 56

Figure 4.6: Example Training Record for Radial Basis Network Using Jerk Profile 57
Figure 4.7: Training Record for Radial Basis Network Using Five Jerk Profiles..... 57
Figure 4.8: Training Record for Radial Basis Network Using Four Jerk Profiles 57
Figure 4.9: Training Record for Feedforward Network Using Spikiness Index..... 58
Figure 4.10: Training Record for Network Trapped in Local Minima 58
Figure 4.11: Training Record for Network Trapped in Local Minima 59
Figure 5.1: Drowsiness Indicator using Jerk Profile #1..... 61
Figure 5.2: Drowsiness Indicator using Jerk Profile #2..... 61
Figure 5.3: Drowsiness Indicator using Jerk Profile #3..... 62
Figure 5.4: Drowsiness Indicator using Jerk Profile #4..... 62
Figure 5.5: Drowsiness Indicator using Jerk Profile #5..... 63
Figure 5.6: Drowsiness Indicator using Jerk Profile #6..... 63
Figure 5.7: Drowsiness Indicator using Jerk Profile #7..... 64
Figure 5.8: Drowsiness Indicator using Jerk Profile #8..... 64
Figure 5.9: Drowsiness Indicator using Spikiness Index #1 66
Figure 5.10: Drowsiness Indicator using Spikiness Index #2 66
Figure 5.11: Drowsiness Indicator using Spikiness Index #3 67
Figure 5.12: Drowsiness Indicator using Spikiness Index #4 67
Figure 5.13: Drowsiness Indicator using Spikiness Index #5 68
Figure 5.14: Drowsiness Indicator using Spikiness Index #6 68
Figure 5.15: Drowsiness Indicator using Spikiness Index #7 69
Figure 5.16: Drowsiness Indicator using Spikiness Index #8 69

LIST OF TABLES

Table 1.1: Reaction Times for Levels of Alertness (Faber, et al., 2003) 3

Table 1.2: PERCLOS, LDBF and Fusion drowsiness detection (Chang, et al., 2005) 9

Table 1.3: Results of Spikiness Index Analysis (Haque and Desai, 2006) 14

Table 2.1: Motion Range of Simulator Base 28

Table 2.2: Simulator Computer Network Architecture 29

Table 2.3: Simulator Hardware 29

ACKNOWLEDGMENTS

The author would like to express thanks to Dr. Moustafa El-Gindy and Dr. Aman Haque for their continuous technical help during the course of this research.

The author would also like to express his gratitude to the Applied Research Laboratory (ARL) of Penn State University and its E&F Graduate Assistant program directed by Dr. Dick Stern.

This thesis was made possible in part by Dr. Aman Haque and his Honda Initiative Grant.

CHAPTER 1: LITERATURE REVIEW OF DRIVER ALERTNESS MONITORING TECHNIQUES

1.1 Introduction

Security and safety on the roadway are major concerns of modern society. Recent studies show driver drowsiness as a major cause of automobile accidents on roadways across the world (Rau, 1996). In this respect, fatigue and monotony are two of the critical factors that decrease driver vigilance and increase risk of injury or death to both the driver and the surrounding public (Faber, 2004). In the United States, the National Highway Traffic Safety Administration (NHTSA) estimates 100,000 crashes reported, 1,550 deaths, and 76,000 injuries (Strohl, et al., 1998) due to fatigue. Economically, this corresponds to $12.4 billion per year in losses due to driver drowsiness (Grace, 1998; Wang, et al., 1996). These numbers highlight the need for research and development of an effective drowsiness detection system for use in heavy trucks and automobiles.

The purpose of this chapter is to review the causes and symptoms of loss of alertness and to make a decision on inputs to evaluate the level of driver vigilance. The next section of this chapter is devoted to the causes of impairment of vigilance. Section 1.3 will present the available techniques for alertness monitoring and rate the effectiveness and practicality of the inputs to the system. Special attention is given to artificial neural network approaches in section 1.4. Finally, a concluding section will choose the type of system for further research based on the findings of the literature review.

1.2 Causes of Alertness Impairment

Operation of any automobile or heavy machinery requires acute attention. In order to safely manipulate the controls of such vehicles, the driver must be able to physically and psychologically stay attentive to the task and environment. Due to the countless factors that present danger to driver judgment, an alertness warning system must be flexible enough to deal with a wide variety of circumstances. Among these factors are sleepiness, fatigue, monotony, distraction and psycho-physiological (drugs, alcohol, emotional) effects. Although all of these factors demonstrate great risk, this review is mainly concerned with sleepiness and fatigue.

1.2.1 Human Sleepiness

Sleepiness and drowsiness are two synonymous terms that are defined by the Merriam-Webster Dictionary as “a very sleepy state; the need

to fall asleep" (2006). It is necessary to understand the mechanisms of sleep as well as its causes. During drowsiness, an individual's awareness of the surrounding environment becomes sporadic (Makeig, et al., 2000). Researchers have investigated human sleepiness for many years and much has been discovered about the process as well as how to monitor alertness. One major sleep research technique is to monitor brain activity using an electroencephalogram (EEG). Using an EEG, researchers measure electrical currents within the neural system of the human brain with sensors placed on the skin. An EEG can show the state of the human brain because the characteristic patterns of current differ for asleep, awake, and anaesthetized states. Correlations between vigilance states (Alert, Relaxed, and Sleepy) and reaction time have been exemplified using an EEG. Table 1.1 displays the average reaction time for selected vigilant states defined by EEG data.

Table 1.1: Reaction Times for Levels of Alertness (Faber, et al., 2003)

Vigilant State	Reaction Time (ms)
Alert	100-400
Relaxed	400-800
Sleepy	800-1200 $\rightarrow \infty$

Ground-breaking work published by Kleitman and Aserinsky (1953) determined that sleep is not a passive state. In fact, sleep consists of two states of Rapid Eye Movements (REM) and non-REM. REM sleep is an active state of sleep with EEG measurements similar to those of an active state (Dement and Kleitman, 1957). Kleitman also created the concept of an internal clock during his research of the natural inclination and timing of sleep.

This internal clock is known as the circadian rhythm. The circadian rhythm is a daily cycle of a drive to sleep due to the timing of one's biological clock. The circadian rhythm shows periods of unintended sleepiness to occur around the times of 6 am and mid-afternoon (Sagberg, et al., 2004).

The other factor that induces sleepiness is a homeostatic influence. An average adult sleeps a little longer than eight hours per night. Research conducted by David Dinges shows that it is not "sleep debt" but a homeostatic factor of continual wakefulness that causes the human body to become sleepy (Dinges, 1995; Dinges, et al., 2001). If one stays awake for more than 18 hours, it has been found that the human body enters a state of decreased performance during simple tasks. The longer one stays awake past 18 hours, the further the decrease in their performance.

1.2.2 Fatigue

"Fatigue" is often mistakenly used as a synonym for "sleepiness". Fatigue combines the psychological and physiological disinclinations to continue simple control tasks or start new ones (Desai and Haque, 2006). This can be caused by numerous factors including sleepiness, but one can suffer from fatigue and not be drowsy (Stutts, et al., 1999). Figure 1.1 presents the key influences on fatigue from both objective and subjective standpoints.

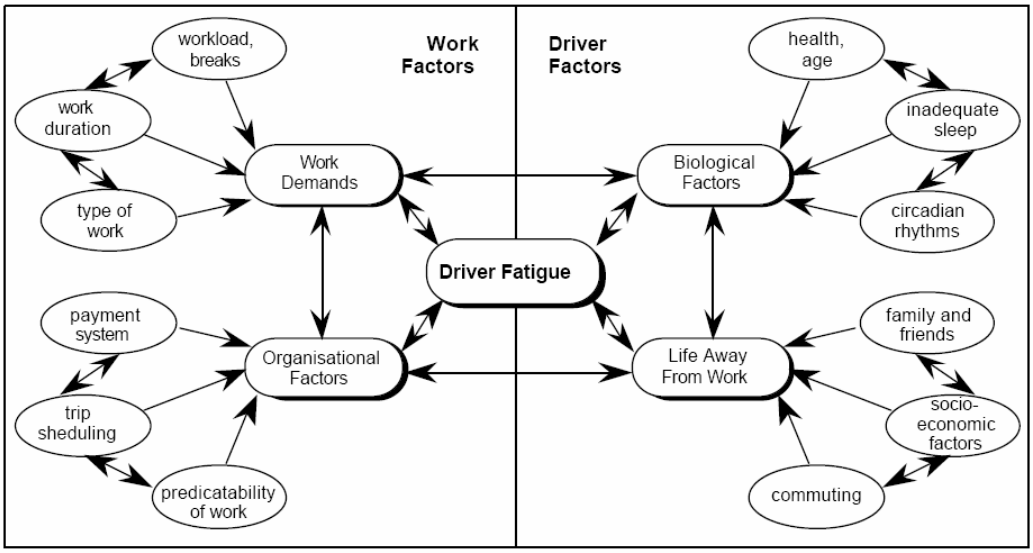

Figure 1.1: Factors Contributing to Vehicle Driver Fatigue (Dawson et al., 2001)

Defining fatigue in the on-road context has never been unanimously accepted within the field of highway safety, but Australia's Fatigue Expert Group (Dawson, et al., 2001) uses both subjective and objective states in its definition:

> "Impaired performance (loss of attentiveness, slower reaction times, impaired judgment, poorer performance on skilled control tasks, increased probability of falling asleep) and subjective feelings of drowsiness or tiredness. Long periods awake, inadequate amount or quality of sleep over an extended period, sustained mental or physical effort, disruption of circadian rhythm… inadequate rest breaks and environmental stress (such as heat, noise, and vibration)"

1.2.3 Monotony

The characteristics of a trip in an automobile also create factors that decrease vigilance. Monotony is an intricate phenomenon that affects drivers' physical and perceptive senses (Brandt, et al., 2004). Monotony is caused by the lack of stimuli, such as a task that is repetitive or requires low amounts of attention. Factors such as noise, vibration, and empty long straight roads create a monotonous environment (Thiffault and Bergeron, 2003).

The effect of such a monotonous environment can lead to a condition known as "highway hypnosis" (Shor and Thackray, 1970). While in a hypnotic state, the lack of stimuli may result in a decrease in driver alertness (Desmond and Hancock, 2001).

1.3 Driver Alertness Monitoring Techniques

Existing approaches for monitoring driver alertness can be divided into three categories as follows:

- Observing the car
- Observing the driver
- Observing the car-driver interface

Car observation can include monitoring lane drift, car speed, yaw rate, etc. Driver observation includes monitoring facial features, eye movements and physiological responses such as an electroencephalogram (EEG) or skin impedance. Car-driver interface observation includes all methods of

measuring driver imparted motions to the car. This can include monitoring steering displacement rate, grip force on the steering wheel, accelerator displacement rate, etc.

1.3.1 Car Observation Systems

Lane departure is by far the most widely used form of car observation. This technique calculates the position of the vehicle within the lane (usually via a vision system) and monitors how this position changes with time. If the system finds the vehicle is leaving the lane (or roadway) a warning is given. AssistWare Technology has developed a product, SafeTRAC, which uses lane departure and boasts one example of a 350 mile trip in which the weather conditions and lane lines were optimal for lane departure recoginition for 99.45% of the trip, and experienced no false positives and no false negatives.

In a study by Jung and Kelber (2005) a lane departure warning system based on the lateral offset of the vehicle with respect to the center of the lane was developed. A linear-parabolic model was created to detect the lane boundaries, and the linear part (up to 30 meters ahead of the vehicle) was used to compute the lateral offset without needing information about the camera angles. Figure 1.2 shows the two sections (linear and parabolic) of the model.

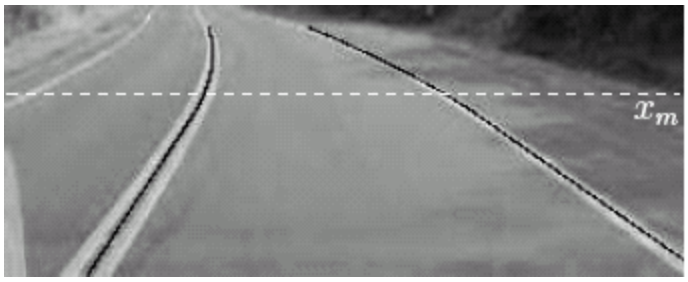

Figure 1.2: Linear and Parabolic Regimens (Jung and Kelber, 2005)

The offset was analyzed across time to detect whether the vehicle approaches the lane boundaries or the offset remains constant. The system was tested with video sequences obtained in different environmental conditions, such as faded lane line painting and various amounts of light, to favorable results.

Other similar methods of lane departure warning have been described by Yasui, et al. (1998), and LeBlanc, et al. (1996). Systems of this type are able to measure and interpret symptoms independent of the driver's physical characteristics. However, there are also several negative aspects. These systems require a large amount of computing power and cannot detect driver drowsiness directly. In addition, systems of this nature may giving false warnings due to a particular driver's style of driving or give late warnings.

1.3.2 Driver Observation Systems

One of the most popular methods used to estimate driver drowsiness is a vision based measurement of the percentage of eyelid closure (PERCLOS) over time. A PERCLOS drowsiness metric was established by Wierwille, et al., (1994) as the proportion of time in a minute that the eyes are at least 80 percent closed. Further work by Dinges and Grace (1998) found

PERCLOS to be both valid and reliable. PERCLOS is used in The Driver Fatigue Monitor (DD850) by Attention Technologies, Inc., making it one of the few drowsiness detection techniques that are commercially available.

Bergasa, et al., (2004) devised a method of real-time monitoring of driver alertness using PERCLOS. An active IR illuminator and software were used to monitor eyelid movements and the pose of the face. The system used PERCLOS, eye closure duration, blink frequency, nodding frequency and face direction as inputs to a fuzzy system. Bergasa validated the method by testing with ten drivers with different light levels. The system was able to work in varying light levels and, using PERCLOS, had a detection percentage of 90% compared to observer measurements. However, when drivers wore eyeglasses the method's performance decreased.

Chang, et al., (2005) used PERCLOS and long blink duration frequency (LDBF) as measurements of driver drowsiness. Chang, et al., defined LDBF as the number of long blinks in which the eye is closed longer than usual. Eye closure was defined as the eye being more than 70% closed. The LDBF and PERCLOS measurements were combined by fuzzy integral to improve the system's performance. This combination of measurements led to 3.3% and 8.3% increase in accuracy over LDBF and PERCLOS, respectively. Complete results of this study are shown in Table 1.2.

Table 1.2: PERCLOS, LDBF and Fusion drowsiness detection (Chang, et al., 2005)

	Samples	Errors	Error Rate (%)	Accuracy (%)
LDBF	122	10	8.2	91.8
PERCLOS	122	16	13.2	96.8
Fuzzy Intergral Fusion	122	6	4.9	95.1

A driver drowsiness detection method was described by Ji, et al., (2004) using remotely located charge-coupled-device cameras equipped with active infrared illuminators to acquire video images of the driver. Various visual cues that typically characterize the level of alertness of a person (eyelid movement, gaze movement, head movement, and facial expression) were extracted in real time and systematically combined to infer the fatigue level of the driver. Ji developed a probabilistic (Bayesian network) model was from known causes of fatigue to model human fatigue and to predict fatigue based on the visual cues obtained. Among the many factors that can cause fatigue, this study used sleep history, Circadian Rhythm, work conditions, work environment, and physical condition. This system is visualized in Figure 1.3.

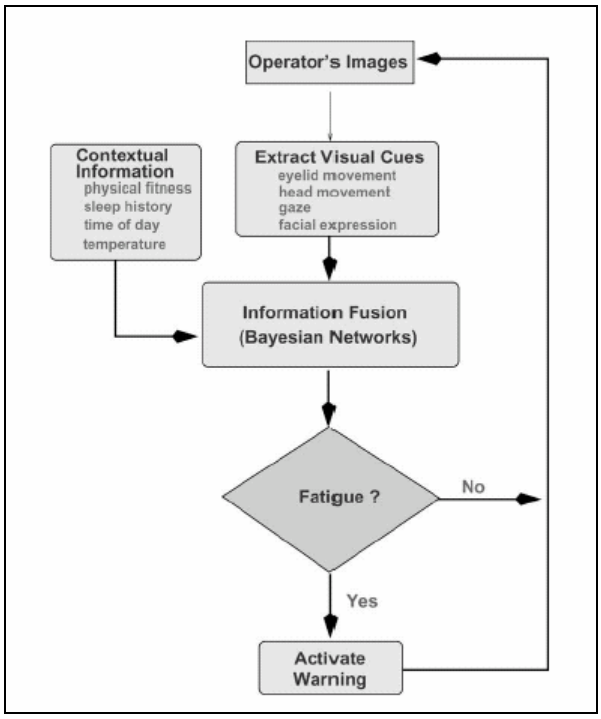

Figure 1.3: Flow Chart for Vision/Context-Based System (Ji, et al., 2004)

The simultaneous use of multiple visual cues and their systematic combination yielded a much more robust and accurate fatigue characterization than using a single visual cue. This system was validated under real-life fatigue conditions with human subjects of different ethnic backgrounds, genders, ages, with/without glasses, and under different light conditions. It was found to be reasonably robust, reliable, and accurate in fatigue characterization. This study manually detected the eyes in a set of 13,620 image stills and used these frames as the correct fatigue identifications. The eye tracker was quite accurate, with a false-alarm rate of 0.05% and a misdetection rate of 4.2% when presented with the 13,620 image stills.

Ueno, et al., (1994) developed a system that uses image-processing techniques to analyze images of the driver's face taken with a video camera. Alertness ratings were based on the number of times eye closure was detected during a specified interval. The system was experimentally validated by driving an actual vehicle and by laboratory simulation. When the alertness ratings from the image processing were compared to brain wave based alertness ratings, a correlation coefficient of 0.77 was obtained, meaning the image processing and physiological responses were strongly relateted.

Several other similar facial/eye image processing based approaches have been described by Tack and Craw (1996), Nakano, et al. (1996), Smith, et al. (2000), Eriksson and Papanikolopoulos (2001) and Kaneda, et al.

(1999). Facial/eye image processing systems do not interfere with driving but the results are dependent on a specific driver (i.e. a driver with glasses versus a driver without). Driver observation methods have the advantage of measuring actual physiological responses to drowsiness. These systems have the disadvantages of using a large amount computing power for image processing.

1.3.3 Car-Driver Interface Observation Systems

Work by Chien, et al. (2003), developed a driver alertness detection method that monitored changes in the driver's grip force on the steering wheel. Steering grip force data was obtained using two resistive force sensors attached to the steering wheel connected to a personal computer with the aid of a data acquisition module. Driving was simulated in a laboratory setting by having subjects perform sessions on vehicle simulator software with a computer game steering wheel. The alertness of the driver was then assessed by a change detection algorithm using the ratio of the probability density based on the mean before a change in steering force and the probability density based on the mean after the change in steering force. The algorithm was successful in detecting changes in steering wheel grip force; however, steering wheel grip force could not be verified as an effective measurement of drowsiness.

Work by Fukuda, et al. (1995), developed a driver drowsiness detection system using the interval of steering adjustment for lane keeping.

Because a real life steering angle waveform contains reaction forces from the road, environmental effects, etc., waveform recognition methods were used to extract steering adjustment measurements alone. The steering interval measurement was normalized to 80 km/h regardless of the actual vehicle speed at that time in order not to impair the real-time performance of the system. The system worked by learning the steering adjustment intervals of drivers according to speed, and the learning time decreases as the vehicle speed becomes higher where the fluctuation in the interval becomes smaller. It also used estimates of steering adjustment data that could not be learned from the normalized data. It then set the drowsiness judgment threshold level according to the values of steering adjustment intervals learned by the system. The system used this threshold level to compare to the driver's steering adjustment interval. If drowsiness occurs, the interval of steering adjustment is prolonged. When tested, the detection algorithm estimated drowsiness with a 15% error as compared to alpha wave (EEG) data and a 7% error as compared to the driver's self-ratings.

A method presented by Haque and Desai (2006) is based on the hypothesis that the time derivatives of forces exerted by the driver on the accelerator and steering wheel can be used to discern different levels of alertness. This technique is novel because it employs multiple inputs to increase the robustness of the system. Their study introduced a parameter, "spikiness index," for the time series data of the force derivatives to quantify

driver alertness. The spikiness index represents the variations from the general trend and the amplitude of the spikes, as shown in Figure 1.4.

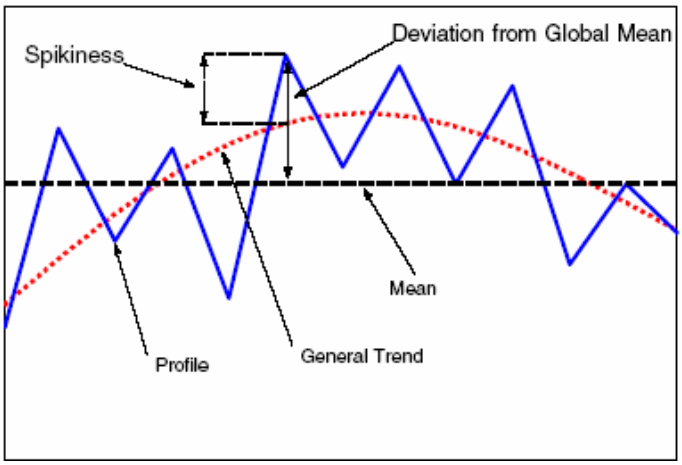

Figure 1.4: Graphical Representation of Spikiness Index (Haque and Desai, 2006)

Haque and Desai hypothesized that the spikiness index decreases as the driver becomes drowsy. To test the theory three drivers performed simulated driving while alert and drowsy, the derivative of the force on the gas pedal was taken and the spikiness index (deviation from the moving average) was computed and is shown in

Table 1.3.

Table 1.3: Results of Spikiness Index Analysis (Haque and Desai, 2006)

	Driver 1		Driver 2		Driver 2	
	Alert (N/s)	Drowsy (N/s)	Alert (N/s)	Drowsy (N/s)	Alert (N/s)	Drowsy (N/s)
1	2.27E-02	6.09E-03	2.67E-02	8.45E-03	1.36E-01	4.23E-03
2	5.00E-02	8.85E-03	9.93E-03	2.00E-02	2.97E-02	2.42E-02
3	3.67E-02	1.73E-02	8.84E-03	1.79E-02	8.88E-02	3.03E-02
4	1.56E-02	4.60E-03	5.33E-03	2.00E-02	6.58E-02	2.16E-02
5	9.02E-03	3.33E-03	11.11E-02	2.00E-02	4.38E-02	8.97E-02
Avg	2.68E-02	8.03E-03	1.124E-02	6.48E-03	7.28E-02	3.40E-02

One of the most unique studies in driver drowsiness detection and warning is the AWAKE project (Bekiaris et al. 2004). The AWAKE system is exceptional because of its multi-sensor approach, using feedback from driver responses and traffic situations to diagnose driver drowsiness. The System for effective Assessment of driver vigilance and Warning According to traffic risK Estimation (AWAKE) is a project of the European Commission intended to diagnose driver alertness impairments in terms of progressive or critical alertness lapses, allowing the driver to avoid a more hazardous situation. The goal of AWAKE is to achieve a correct diagnosis level of 90% and a false alarm rate below 1 % in all highway scenarios. Figure 1.5 shows a flow chart for the AWAKE system.

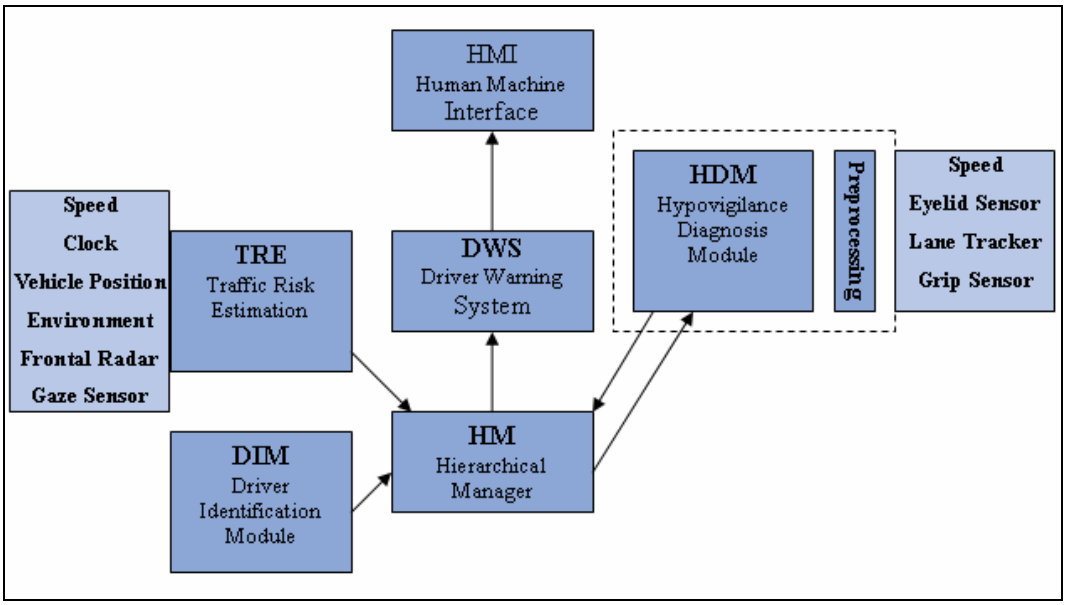

Figure 1.5: Flow Chart for AWAKE System (Bekiaris et al. 2004)

A Hypo-vigilance Diagnosis Module (HDM) detects drowsiness in real-time. Based on an artificial intelligence algorithm, this module will monitor eyelid behavior, steering grip forces, and lane keeping performance.

A Traffic Risk Estimation module (TRE) assesses the traffic situation and the involved risks. It monitors data from an enhanced digital navigational map, positioning system, anti-collision radar, vehicle speed, and the driver's gaze direction.

The Hierarchical Manager (HM) co-ordinates the other system components and hosts the AWAKE warning strategy (Bekiaris et al. 2004). According to this diagnosis, the AWAKE warning strategy is as follows:

- If driver is awake, only imminent collision and imminent speed warnings can be activated
- If driver may be drowsy, all levels of traffic risk warnings can be activated
- If driver is drowsy two different drowsiness warnings and traffic risk warnings can be activated

Car driver interface systems have the advantage of being completely un-intrusive to driving. They can be implemented without the driver being aware of the system. They also use less computing power than other image processing based systems. Like car observation systems, car-driver interface observation systems have the disadvantage of not being able to directly monitor driver drowsiness.

1.4 Alertness Prediction Using Artificial Neural Networks

Generally speaking, an artificial neural network (ANN) consists of a set of interconnected processing elements (called neurons) which can exhibit

complex global behavior. Originally, this technique was inspired by simplified models of the human brain, hence its name. The true power of artificial neural networks is their ability to recognize patterns. Considerable work has been done to develop algorithms to train neural networks to detect patterns in data sets (Chen, 1990; Carpenter, 1989; Kohonen, 1988). Artificial neural network computations are carried out in parallel (Carpenter and Grossberg, 1987) and thus can be very fast. If adequate inputs for a network can be determined (from car, driver or car-driver interface observations), artificial neural networks show promise for alertness prediction.

A driver drowsiness detection process based on an artificial neural network (ANN) was described by Sayed and Eskandarian (2001). Steering angle signals were preprocessed and presented to the ANN, which classifies them into drowsy and non-drowsy driving intervals. The neural network architecture used in this study was a three-layer feed forward network connected by full synapses. The input layer had eight neurons corresponding to the eight-dimensional input vector, the hidden layer has 22 neurons (the number of neurons in this layer was selected on the basis of a sensitivity analysis) and the output layer has two neurons corresponding to two possible outcomes, i.e. drowsy and non-drowsy. Sayed and Eskandarian used the error back-propagation learning algorithm to train the network. The process was validated by an experiment conducted at the highway-driving simulator at the Turner Fairbank Highway Research Center. Twelve subjects (half male, half female) between ages 25 and 35 were used in the experiment. Subjects

drove a 20 mile (36 km) rural loop with both straight and curved sections under different levels of sleep deprivation. Data was classified as drowsy if the driver was sleep deprived by continuous wakefulness or the driver fell asleep and non-drowsy otherwise. The network classified 89.9 percent of the test data into the correct drowsy and non-drowsy classifications selected by the researchers. During simulation in which the subject fell asleep and crashed the vehicle, the ANN detected drowsy driving an average of 3.5 minutes before the crash occurred.

A study by Wilson and Bracewell (2000) created an artificial neural network with EEG inputs to detect drowsiness. The input to this ANN system was a modified feature vector composed of the associated wavelet representations of the EEG data at different scales. The first stage filtered the incoming EEG signal, capturing regions of interest as wavelet coefficients and power spectrum estimates. The filter bank filters into low pass (0-8 Hz) and high-pass regions and then into the regions associated with simplified alpha, theta, K complex, and delta characteristics. The alpha wave depicting the early signs of drowsiness is most predominant in the 8-12 Hz spectral range. The theta wave is characterized roughly as 3-7 Hz. The sleep spindles and K complex are prevalent at 12-14 Hz. Delta sleep is defined as 0.5-2 Hz. This set of wavelet coefficients was combined with power spectrum estimates to produce a modified feature vector used as an input to the ANN. The output of the neural network was a binary decision as to whether the EEG represents

an alert state or a drowsy state. A flow chart of the system is shown in Figure 1.6.

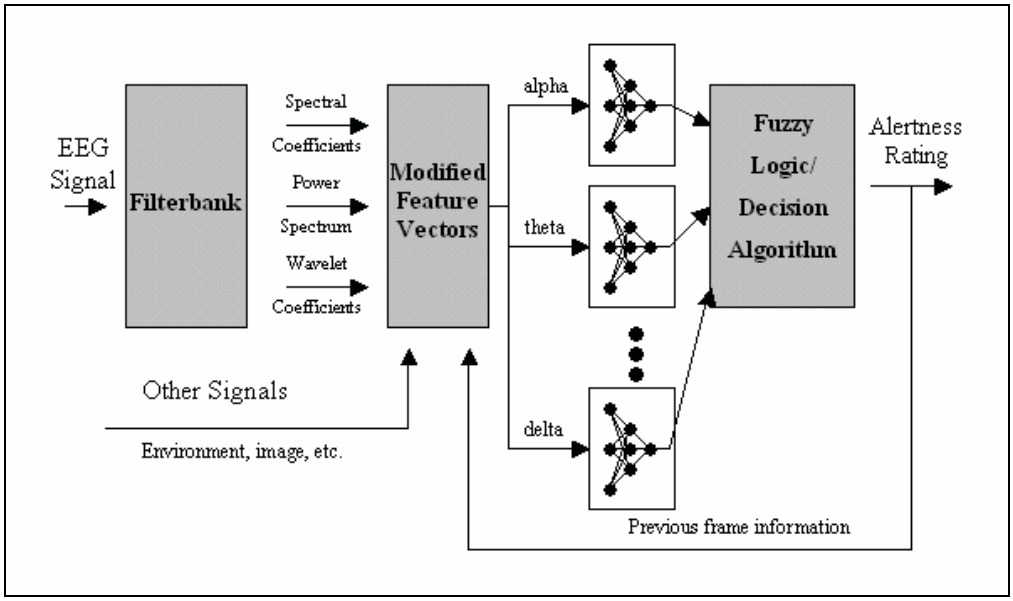

Figure 1.6: Flow chart for EEG Analysis System (Wilson and Bracewell, 2000)

The network was trained with synthetic data patterns of discrete input values mapping the outputs of the spectral tuning networks to the alertness level assignments ranging from 1 (very alert) to 7 (sleep). In efforts to simulate EEG noise that might actually occur due to chemical intake (such as coffee), the test dataset was supplemented with additional levels of noise. The artificial neural network model was 99% correct and all errors were misses. The artificial neural network model gave no false alarms.

Andreeya, et al. (2004), proposed a drowsiness detection system based on vibration characteristics of the driver's body. The driver's body was studied as a linear time-variant (LTV) structure of springs and dampeners (Figure 1.7).

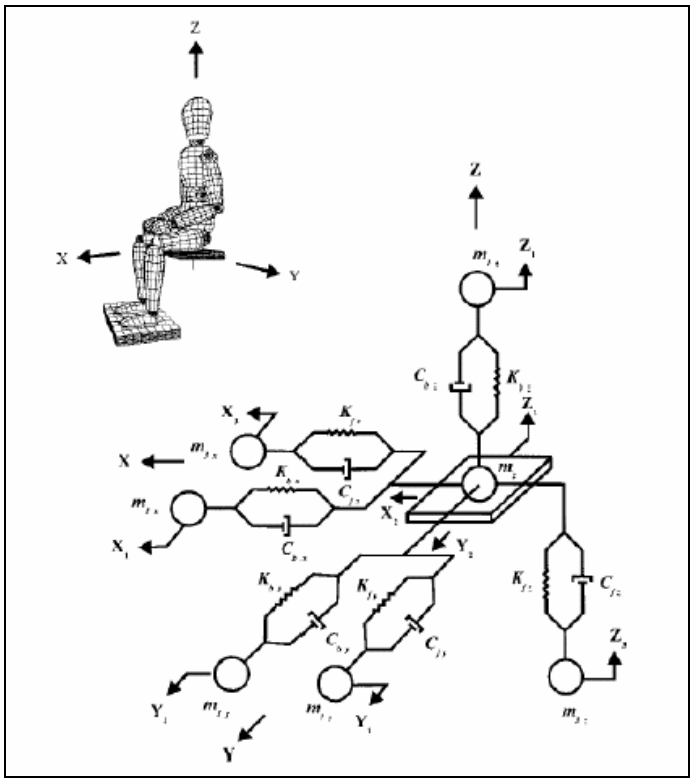

Figure 1.7: Spring-Damper Representation of Human Body (Andreeya, 2004)

Vibrations traveling from the car seat through the body towards the head are affected by the spring-damper structure. The hypothesis of Andreeya, et al., (2004) was that the filtration effects of the body are dependent on the driver's state of sleepiness, and can therefore be used as indication of driver drowsiness. To generate the input and desired signals of the driver's upper body (the unknown plant), tri-axial accelerometers were placed on the driver's seat and on the driver's head. The normalized least-mean square (LMS) algorithm was used for plant identification and generation of weight coefficients for the system. The weights were pre-normalized to have zero mean, and unit variance distributions. Separate coefficients were generated for the "awake" and "asleep" states of the subject and then used to train a neural network to classify the driver's condition. A feed-forward artificial

neural network, with 140 hidden units was used for classification. The back-propagation algorithm was used for training. The experiment, tested on eight subjects, was conducted on sleep-deprived individuals for the “sleep” state and on fully awake individuals for the “awake” state. When trained and tested on the same subject, the system detected “sleep” and “awake” states of the driver with a success rate of 95%. When the system was trained on three subjects and then retested on a different fourth subject, the classification rate dropped to 90%.

Vuckovic, et al., (2002) presented a method for classifying alert versus drowsy states from one second sequences of full spectrum EEG recordings from an arbitrary subject as the input to an artificial neural network (ANN) with two discrete outputs: drowsy and alert. The study used the following definitions: The “alert” state refers to an EEG recording with the occipital alpha rhythm present and the “drowsy” state refers to a drowsy EEG recording (i.e. presence of slow eye movement with the occipital alpha rhythm, a decrease in the amplitude, and/or frequency of the alpha rhythm, low amplitude activity at the central and posterior EEG channels preceding the Stage 1 sleep) and the Stage 1 sleep EEG recording. Two experts in EEG interpretation visually inspected the data and provided the necessary expertise for the training of an ANN. Three artificial neural networks were used: a linear network trained by Widrow-Hoff algorithm; a feed-forward neural network trained with the Levenberg–Marquardt (LM) rule; and a self organizing network trained with the Learning Vector Quantization (LVQ) rule.

It was shown that the LVQ neural network gives the best classification compared with the other two networks. Classification properties of LVQ were validated using the data recorded in 12 healthy volunteer subjects, yet whose EEG recordings have not been used for the training of the neural networks. The statistics were used as a measure of potential applicability of the LVQ: the t-distribution showed that matching between the human assessment and the network output was 94.37 ± 1.95%. This result suggests that the automatic recognition algorithm is applicable for distinguishing between alert and drowsy state in recordings that have not been used for the training.

Work by Hayashi, et al., (2005) described a detection method of driver's drowsiness with focus on analyzing biological signals and driving performance data. As the input data, sympathetic nerve activity, parasympathetic nerve activity, pulse rate, Lyapunov exponent, and steering instability were derived from driver's pulse wave and steering data. Additionally, the score of Epworth Sleepiness Scale (a questionnaire used to determine the level of daytime sleepiness) was also used. To analyze the indexes in consideration of the individual differences, artificial neural networks were used. A flow chart summarizing the method by Hayashi et al. (2005) is shown in Figure 1.8.

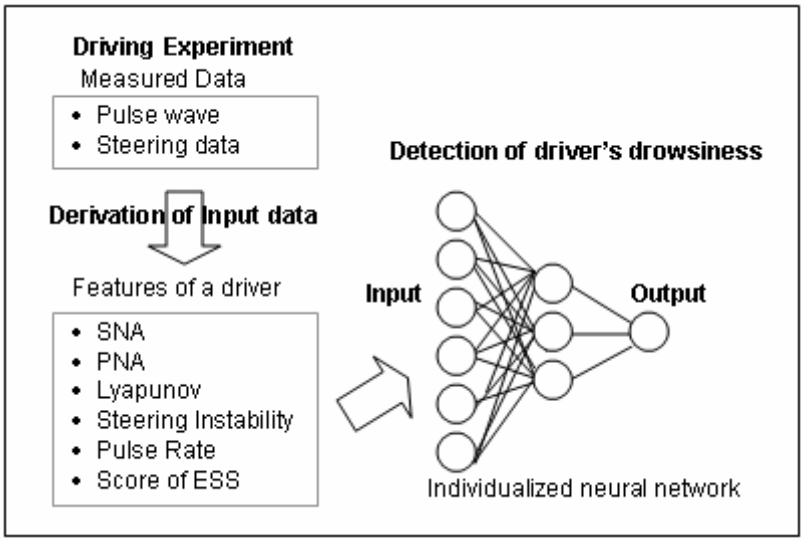

Figure 1.8: Biological and Driving Signal System (Hayashi et al., 2000)

Two detection methods of driver's drowsiness were proposed in this paper: individualized drowsiness detection (learning each driver's feature on each network) and individualized drowsiness detection with categorization (categorizing drivers with sympathetic nerve activity before their data were input into the networks). To test the system, pulse wave and steering data were gathered from six individuals using a driving simulator. Individualized drowsiness detection averaged an 88% detection rate and individualized drowsiness detection with categorization averaged an 85% detection rate.

Carswell and Chandran (1994) describe a method for the detection of abnormal vehicle trajectories. It was hypothesized by Carswell and Chandran (1994) that abnormal trajectories are indicative of drunk or sleepy drivers. Figure 1.9 shows possible examples of these trajectories.

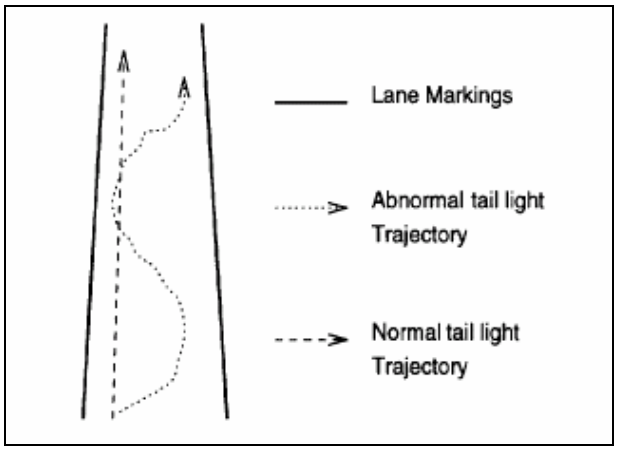

Figure 1.9: Normal and Abnormal Trajectories (Carswell and Chandran, 1994)

The system coupled optical flow extraction of vehicle velocities with an artificial neural network classifier. A single feature of the vehicle, e.g., a taillight, was isolated and the optical flow was computed only around this feature rather than at each pixel in the image. The velocity fields were accurately extracted using a modification of the basic optical flow method**.** The training and testing data sets each contained approximately 50% normal and 50% abnormal trajectories where abnormal trajectories represented a vehicle whose path was oscillating around the correct trajectory (Figure 4.3). Absolute deviations for abnormal trajectories were overall greater than for normal trajectories but the normal set still allowed some deviation. The ANN was used to classify the vehicle trajectories as either normal or abnormal. The artificial neural network was trained with the back-propagation learning algorithm and converged after 100,000 iterations. When tested with the 40 test sequences, the neural network classified the trajectories with 100% accuracy.

Despite the differences in the measurements used as inputs in these studies, artificial neural networks show great potential for classifying driver behavior. When using an artificial neural network, a designer has many numerical training algorithms to learn how to distinguish alert driving from non-alert driving available. However, artificial neural networks have the disadvantage of needing a large amount of data sets for adequate training.

1.5 Literature Review Conclusions

This review has described significant causes of driver alertness deficiency, including fatigue, sleepiness and monotony. So far, the research and development on driver alertness warning systems has yielded significant results, yet very few commercial products are available. Criteria for an ideal driver alertness monitoring system that could be commercially viable are given by Desai and Haque (2006) as:

- Non-intrusive monitoring that will not distract the driver or compromise privacy.
- Real-time monitoring to ensure accuracy and speed in detecting lowered levels of driver alertness.
- System performance that is independent of environmental conditions (traffic, landscape, weather, and darkness).
- Low unit and operation (including data processing) costs.

Using these criteria guidelines, the introduction of a driver alertness warning system prototype is a realistic goal within the near future. Using these

guidelines and the conclusions from the review of different types of input, car-driver interface analysis has been chosen for this study. Simple sensors (compared to EEG or image processing) can be used for data acquisition and the driver is unaware of their presence. Artificial neural networks will be used because of the vast number of different types of systems that have proven successful to other researchers.

CHAPTER 2: DRIVER ALERTNESS EXPERIMENT AT THE PENN STATE TRUCK DRIVING SIMULATOR

2.1 Overview of Simulator Architecture

To collect data sets from sleep-deprived drivers, a driving simulator was used. Driving simulation has been used by Chieh et al. (2003), Sayed and Eskandarian (2001), and Hayashi et al. (2005) to test driver alertness monitoring systems. Simulated driving has its limitations; for example the Penn State Truck Driving Simulator has a low maximum frequency response, meaning it cannot provide the driver the feeling of road vibration. Driving simulation is a constantly expanding field and while no simulator is perfect simulated driving is best for an experiment of this nature because there is little to no risk of injury or property damage.

The Pennsylvania State Truck Driving Simulator (PTDS), shown in Figure 2.1, is the product of continued work and development that began in 1997 with the undertaking of the 2TS (Truck Training Simulator) project by a

consortium of four companies, Moog, Inc., Systems Technology, Inc. (STI), Mack Trucks, and Renault (Delahaye and Kemeny, 1999).

Figure 2.1: The Pennsylvania State Truck Driving Simulator

The simulator driver station consists of a Mack Trucks CH600 series truck cab mounted on a six-degrees-of-freedom (roll, pitch, yaw, surge, lateral, and heave) motion platform by Moog, Inc. The motion base has a small frequency range (up to 15 hz), but reacts sufficiently to produce realistic accelerations of a truck and has a range of motion listed in Table 2.1.

Table 2.1: Motion Range of Simulator Base

DOF	Minimum	Maximum
Roll (Degrees)	-29	29
Pitch (Degrees)	-33	33
Yaw (Degrees)	-29	29
Surge (m)	0.381	-0.381
Lateral (m)	0.381	-0.381
Heave (m)	0	0.4752

Three visuals provided a 130° wide by 35° high front view and two rear views of the driver and passenger sides. The simulator also has an amplifier that sends sound cues to the cab to simulate road, traffic and engine noises. In addition, a compressed air line allows for the use of the air horn, vertical adjustment of the driver's seat, and the parking break light to turn off when the appropriate button is pressed.

The functions of the truck simulator are controlled via a network of seven computers. The details of this network are shown in Table 2.2.

Table 2.2: Simulator Computer Network Architecture

Name	Functions(s)	Computer Model
Paris	Host	Dell Dimension 4100 (dual 200 MHz)
Lyon	Dynamics, Cabin I/O	Dell OptiPlex Gxpro (dual 200 MHz)
Toulouse	Sound	Dell Dimension 4100 (800 Mhz)
Grenoble	Center Visual	Dell Dimension 4100 (1000 MHz)
Marseille	Right Front Visual	Dell OptiPlex Gxpro (dual 200 MHz)
Nantes	Left Front Visual	Dell Dimension 4100 (900 MHz)
Bordeaux	Right Rear Visual	Dell Dimension 4100 (800 MHz)
Avignon	Left Rear Visual	Dell Dimension 4100 (800 MHz)

A list of the simulators hardware components is presented in Table 2.3.

Table 2.3: Simulator Hardware

Hardware	Manufacturer	Model
Rear Projectors (2)	InFocus	LP260
Front Projectors (3)	InFocus	LP435Z
Motion Platform	Moog, Inc	170E122A
Cab	Mack Trucks	CH600 series
Rear Screens (2)	Da-Lite	Perm Wall (64" x 84" viewing area)
Front Screens (3)	Da-Lite	Fast Fold (68" x 92" viewing area)
Ethernet switch	3-COM	Super Stack II – 3C16611

Two software components make up the real-time driving simulator (Hoskins, 2002). Vehicle Dynamics Analysis Non-Linear (VDANL) is the vehicle dynamics simulation model used by the PTDS. VDANL was developed for the National Highway Transportation Safety Administration during the mid 1980's (Christos and Heydinger, 1997). Detailed descriptions of VDANL's mathematical models are provided in volumes II, III, and IV of "Analytical Modeling of Driver Response in Crash Avoidance Maneuvering" (Allen et al, 1998). SCANeR© II, developed by Renault, is the software package that controls all the processes used in the interactive simulation (Hoskins, 2002).

The PTDS has undergone extensive validation. Work by Christos and Heydinger (1997) studied the 1994 Ford Taurus model used in VDANL and VDM RoAD, along with experimental test data, to validate each of these models. This study found the simulations predicted vehicle responses well in the linear range.

2.2 Driving Scenario Development

Experiments performed using the PTDS requires the ability to program and develop driving scenarios. Scenarios contain all of the visual and audible stimuli, Traffic, terrain specifications and data collection commands.

Figure 2.2: View from Truck Cab during Simulation

A driving scenario was created with the SCANeR© II program "Mice" following directions given by Hoskins (2002). First, a terrain was selected. Terrain profiles contain the roadway and scenery information used by the simulator. The terrain profile "Mountain" (Figure 2.2) was selected because it contains a four-lane divided highway and it is the appropriate length (roughly 20 minutes to drive across the highway section). This terrain also requires the driver to perform actions such as accelerating and braking for grade changes, lane changing, and left and right hand turning. Figure 2.3 shows the map of this terrain profile and route used during the experiment.

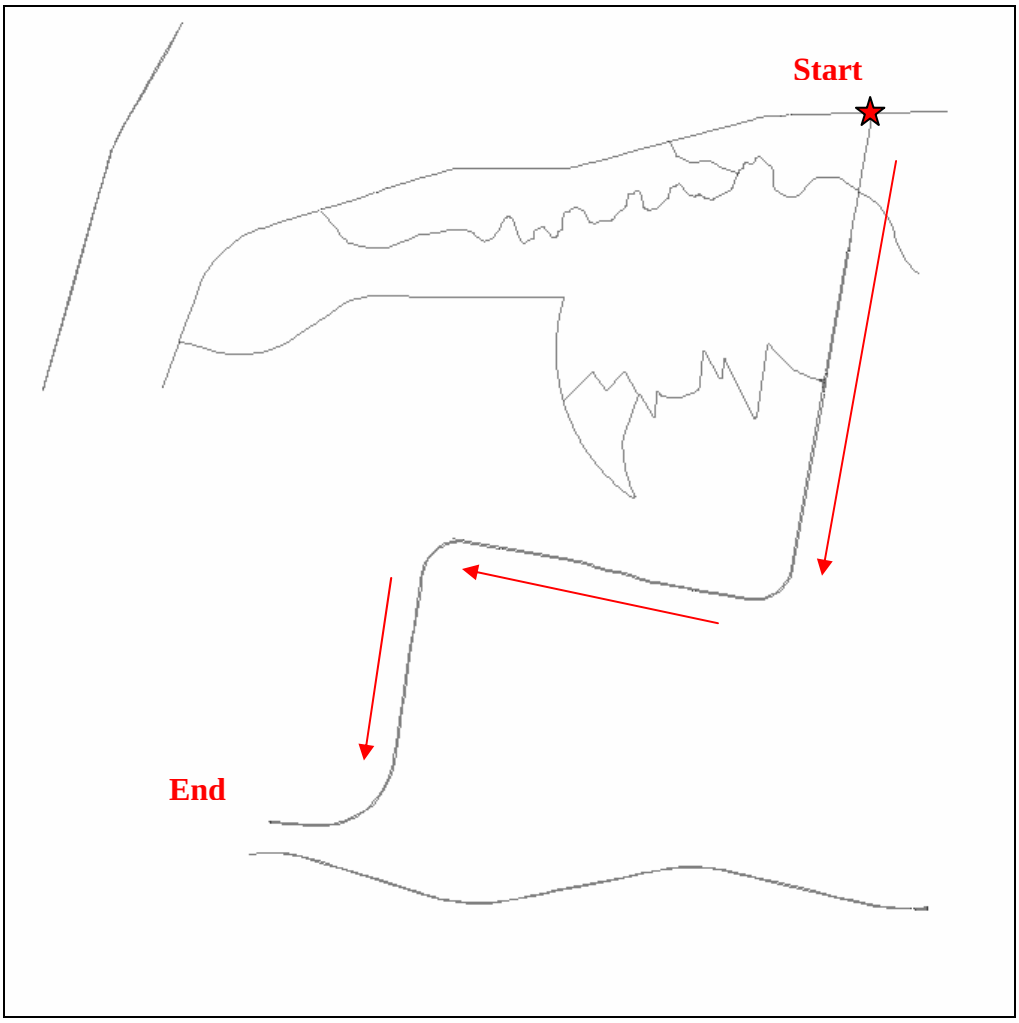

Figure 2.3: Map of “Mountain” Terrain Used for Driving Scenario

Once the terrain was selected, the traffic of the scenario was inserted. Traffic files contain information such as the vehicles present in the simulation, vehicle positioning and behavior. Figure 2.4 shows the traffic setup window.

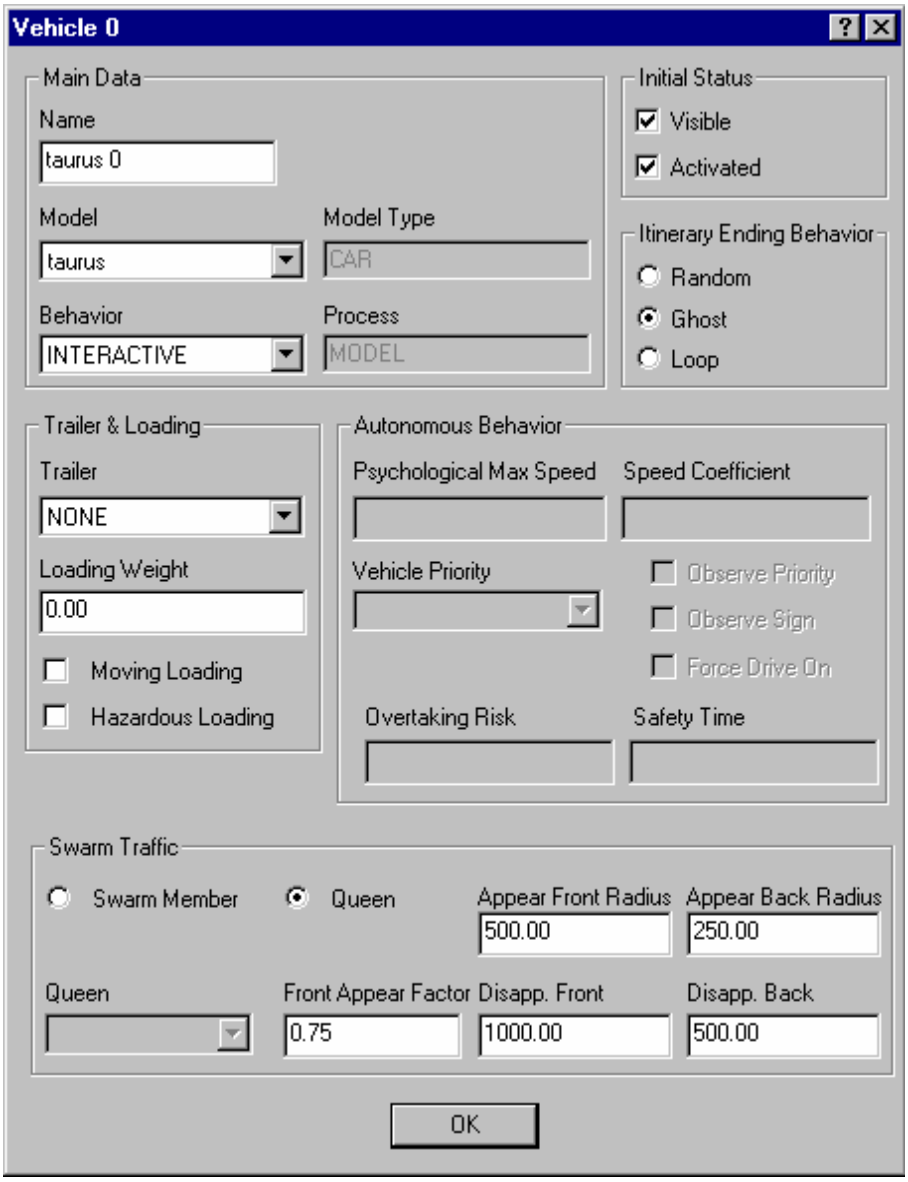

Figure 2.4: Simulated Vehicle Setup

The only traffic used during the experiment was the interactive vehicle. The interactive vehicle is the vehicle that is controlled through the control inputs of the simulator cab. A dynamic model of a Ford Taurus was used because it is a common vehicle that most drivers would feel comfortable operating. The vehicle is also named and given initial status as “visible” and “activated”. Once the vehicle has been created it can be placed in the

desired starting location (Figure 2.3). Traffic/vehicle information is saved in as an addition file (*.trf) in the same directory as the scenario file (*.sc).

There is a large selection of variables that can be recorded during any given simulation, including driver inputs, vehicle responses and scenario events. To record data, the variables were specified separately within a scenario file using the Mice program. The first step to recording data with the simulator is to create an event with a condition that specifies when the recording should begin. For this experiment the data was recorded the entire time, thus the "IF" condition was set to "isScenarioBeginning". Next, actions are created to save specific parameters to export channels. The channel numbers determine the column that the data for the parameters are written to within the output file. The parameters "ScenarioClock", "SteeringWheel", "AcceleratorPedal", "Speed", "SpeedLimit", and "LaneLateralShift" were recorded. In addition, each action specifies the vehicle that the action applies to. Figure 2.5 shows the complete list of rules used to record data.

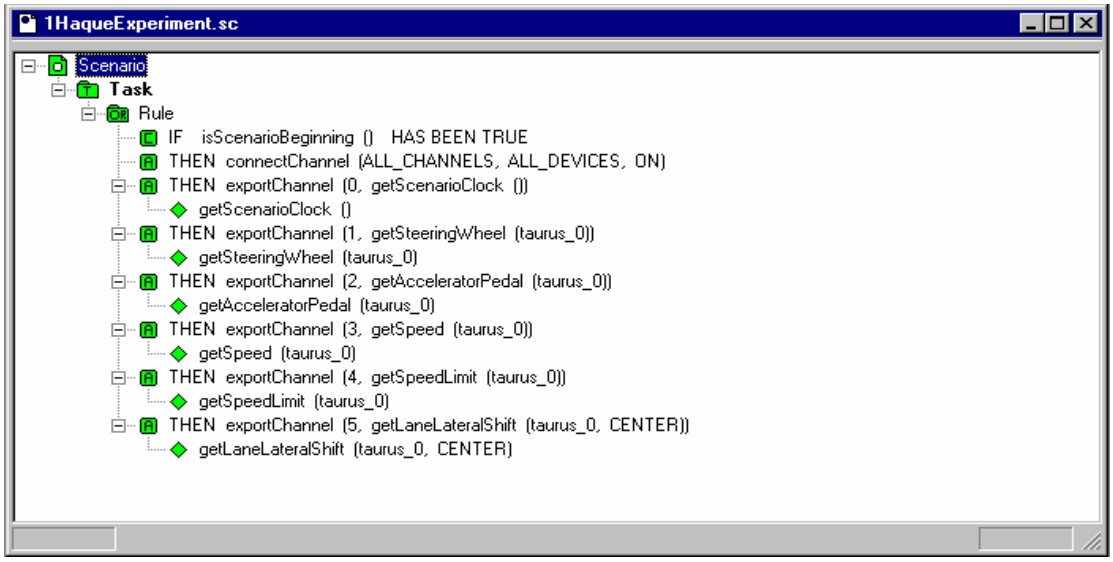

Figure 2.5: Mice Window Showing Data Recording Tasks

2.3 Experimental Procedures

A pool of volunteers was selected to participate in the experiment. The participants were multiethnic and between 20 to 30 years old. Both males and females were represented. Potential volunteers were first screened by a physician to certify that they had no known medical history of adverse effects (mental or physical) due to sleep deprivation. In addition, the volunteers were asked the following questions:

1. Are you feeling well enough to intermittently drive a simulated vehicle for 24 hours?
2. Did you get sufficient sleep last night?
3. Have you had any alcohol to drink in the last 12 hours?
4. Have you taken any medications such as cold pills, allergy pills, anxiety or depression pills that could affect your ability to drive?

Answers of “no” to questions 1 and 2 or answers of “yes” to questions 3 and 4 resulted in disqualification of the candidate.

During each experiment, a group of two participants remained awake at The Pennsylvania State Truck Driving Simulator for 24 hours. The experiment began at 6 pm and ended at 6 pm the next day. During the experiment, the first participant drove for roughly 20 minutes, and then both participants took a 30-minute break. Next, the second participant drove for roughly 20 minutes, and then both participants took another 30-minute break. In addition, the participants were given meal breaks. The participants were instructed to follow normal driving procedures, such as following the speed

limit and maintaining lane position. For each of their 20-minute runs, the participant was asked to rank his or her own perceived drowsiness level from 1 (most drowsy) to 10 (wide awake). While the participants drove, the administrator of the experiment commented on the participants driving noting any crashes, lane drifting or other mistakes. Four experiments were performed for a total of eight participants.

2.4 Data Recording

When the simulation is ended, the data recorded are saved as a binary file containing the data specified in the Mice Window (Figure 2.5). The files created by the simulation software use the naming scheme “scenario name_day_month_year_time.bin”. The binary file is written to the D:/cats/data/record directory on the host computer “Marseille”. The binary data files created by the simulator do not follow a traditional format, making it necessary to use a binary to ASCII converting program provided by Renault (Hoskins, 2002). The binary to ASCII conversion software (on sound computer “Toulouse”) creates delimited text files with columns of data for each “exportChannel” action in the specified in Mice. The delimited text files can then be imported into MATLAB for further analysis.

CHAPTER 3: ARTIFICIAL NEURAL NETWORKS ARCHITECTURE AND TRAINING

3.1 Introduction

Artificial neural networks (ANN) are systems of interconnected elements, called neurons, which operate in parallel. They are inspired by biological nervous systems, hence their name. Artificial neural networks are used to map a set of inputs, P, to a set of outputs, Y. Originally proposed by McCulloch and Pitts (1943), the basic element of the ANN is the neuron (Figure 3.1)

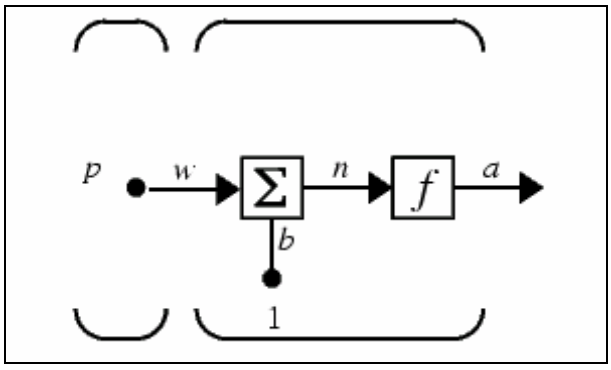

Figure 3.1:Diagram of Neuron

The input p is transmitted through a connection that multiplies its strength by a weight, w. Then a bias b is added to the weighted input. This gives the linear equation

$$n = wp + b \qquad \text{(Eq. 3.1)}$$

The parameter n is used as the argument for a transfer function, f. The result of the transfer function is the output, a.

A single neuron is not able to approximate the behavior of complex systems. Neurons are arranged in parallel to increase the potential of the ANN. A common network model is the feed-forward ANN, shown in Figure 3.2.

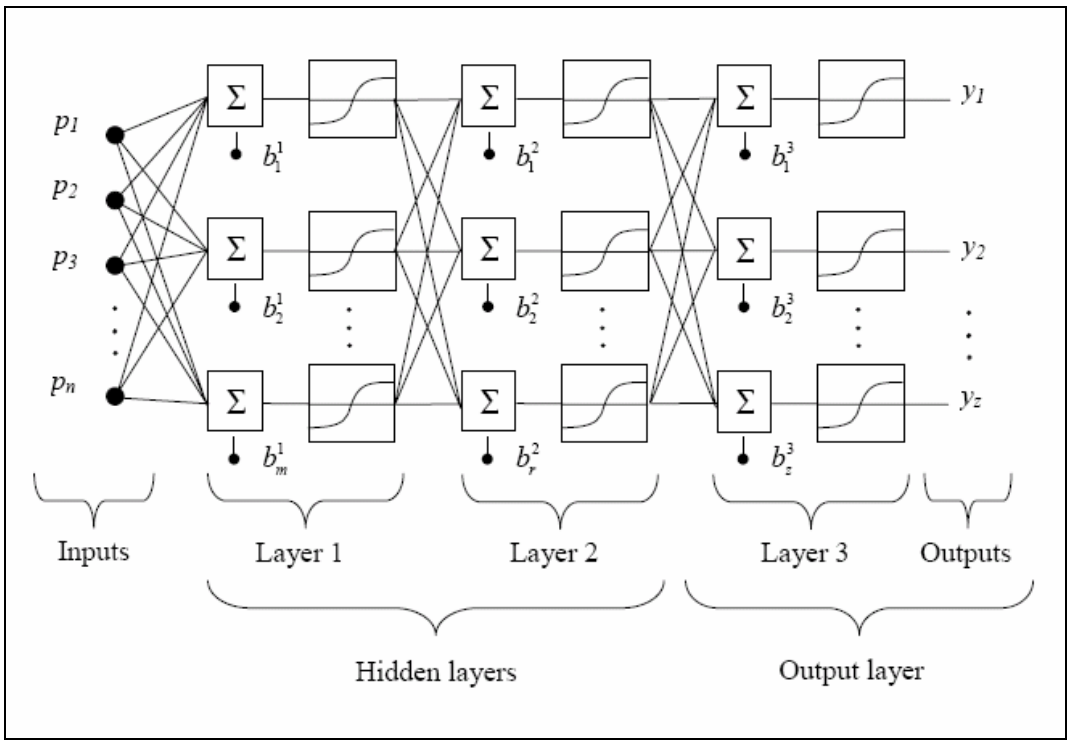

Figure 3.2: Diagram of a Three-Layer Feed-forward ANN

At the first layer of the network, each input is multiplied by a corresponding weight at each neuron, and then a bias is added. This sum is used as an input to a transfer function. The output of the transfer function is then used as an input for the next neuron layer. This parallel structure lends itself well to matrix algebra, and in turn, MATLAB. The inputs are represented as a column matrix with the form

$$\{P\} = \begin{bmatrix} p_1 & p_2 & \cdots & p_n \end{bmatrix}^T \quad \text{(Eq. 3.2)}$$

The weights for each layer can be expressed as a matrix with the same number of columns as inputs and the same number of rows as neurons in the layer with the forms

$$[W]^1 = \begin{bmatrix} w^1_{1,1} & w^1_{1,2} & \cdots & w^1_{1,n} \\ w^1_{2,1} & w^1_{2,2} & \cdots & w^1_{2,n} \\ \vdots & \vdots & \ddots & \vdots \\ w^1_{m,1} & w^1_{m,2} & \cdots & w^1_{m,n} \end{bmatrix}$$

$$[W]^2 = \begin{bmatrix} w^2_{1,1} & w^2_{1,2} & \cdots & w^2_{1,n} \\ w^2_{2,1} & w^2_{2,2} & \cdots & w^2_{2,n} \\ \vdots & \vdots & \ddots & \vdots \\ w^2_{r,1} & w^2_{r,2} & \cdots & w^2_{r,n} \end{bmatrix} \quad \text{(Eq. 3.3)}$$

$$[W]^3 = \begin{bmatrix} w^3_{1,1} & w^3_{1,2} & \cdots & w^3_{1,n} \\ w^3_{2,1} & w^3_{2,2} & \cdots & w^3_{2,n} \\ \vdots & \vdots & \ddots & \vdots \\ w^3_{z,1} & w^3_{z,2} & \cdots & w^3_{z,n} \end{bmatrix}$$

The biases for each layer can be expressed as a column matrix with the same number of rows as neurons in the layer with the forms

$$\{B\}^1 = \begin{bmatrix} b^1{}_1 & b^1{}_2 & \cdots & b^1{}_m \end{bmatrix}^T$$
$$\{B\}^2 = \begin{bmatrix} b^2{}_1 & b^2{}_2 & \cdots & b^2{}_r \end{bmatrix}^T$$
$$\{B\}^3 = \begin{bmatrix} b^3{}_1 & b^3{}_2 & \cdots & b^3{}_z \end{bmatrix}^T \quad \text{(Eq. 3.4)}$$

The output of the network is a column matrix with the form

$$\{Y\} = \begin{bmatrix} y_1 & y_2 & \cdots & y_z \end{bmatrix}^T \quad \text{(Eq. 3.5)}$$

The number of neurons in the output layer is always equal to the number of outputs. The number of and the number of neurons in the hidden layers are arbitrary.

The transfer functions for each layer are also arbitrary. The hidden layers often use a function that has an output between zero and one. This way the neuron can be turned "off" and "on" as appropriate. One transfer function to accomplish this is the MATLAB hard limit, shown in Figure 3.3.

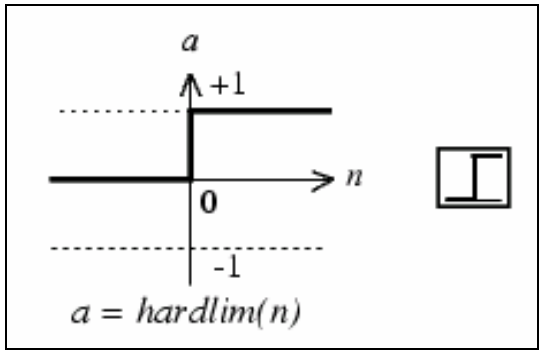

Figure 3.3: MATLAB Hard Limit Function

Some training algorithms require the transfer functions to be differentiable. The log-sigmoid function (Figure 3.4) is used in these cases.

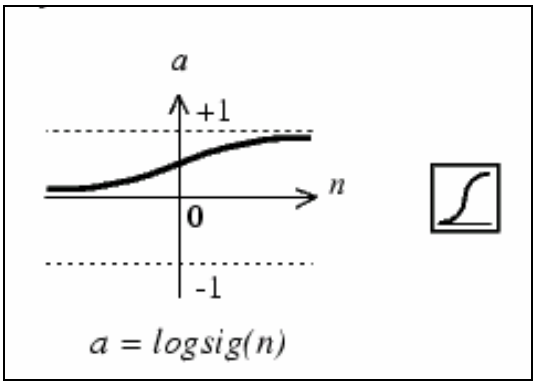

Figure 3.4: MATLAB Log-Sigmoid Function

The log-sigmoid function is expressed as

$$a = \frac{1}{1 - e^{-n}} \qquad \text{(Eq. 3.6)}$$

The "best" network architecture depends on the type of problem the network is being used to represent. Sigmoid transfer functions can be used to represent non-linear functions or pure linear functions can be used for linear mapping. The number of hidden layers and the number of neurons in each layer can be increased to create a more powerful ANN. These parameters are chosen to meet design criteria, usually low summed squared error and a low number of training iterations to convergence.

3.2 Artificial Neural Network Training with Back Propagation

Supervised training uses a training algorithm to adjust the biases and weights to match the artificial neural network's output to a set of target data for a given input pattern. Back-propagation (Rumelhart et al., 1986) is the most widely used ANN training algorithm for multilayer feed-forward networks.

This is algorithm is easy to understand and can solve many minimization problems. The simplest form of back propagation updates the network weights based on the gradient of the sum squared error,

$$\Delta w_{ij} = -\alpha \nabla E \qquad \text{(Eq. 3.7)}$$

$$0 < \alpha \leq 1$$

The algorithm is stopped when the error reaches an acceptably small amount. Additional conditions are usually added to stop the algorithm after a certain number of iterations (called training epochs) or when then gradient has become sufficiently small (i.e. successive steps will no longer reduce error). The parameter α is called the learning rate and, if chosen carefully, decreases training time without loosing stability.

Although gradient descent methods are very popular, several situations exist where problems can arise. A large learning rate can produce an overshoot, where the algorithm missed the minimum value. Conversely, when the gradient becomes small the updates to the weights also are small. This can cause the algorithm to move very slowly through flat regions. The learning rate, α, can be chosen to help alleviate these problems, but selecting an appropriate value can be difficult.

Many algorithms have been proposed to deal with this problem by adapting the learning rate during training. These algorithms can be divided into global and local adaptation. Global adaptation make use of the knowledge of the state of the entire network (e.g. the direction of the previous weight-step) to modify global parameters, whereas local strategies use only

weight-specific information (e.g. the partial derivative) to adapt weight specific parameters (Riedmiller and Braun, 1993). Besides being more memory efficient, local adaptation is better suited for parallel computing.

The Resilient Back Propagation Method (RPROP) introduced by Riedmiller and Braun (1993) avoids the issues of stability while being very memory efficient. The RPROP algorithm deviates from most other methods by the fact that the sizes of the updates to the weights are not determined by the gradient size. Individual weights, ω_{ij}, are updated by a value, Δ_{ij}, which is determined by the following rule:

$$\Delta_{ij}^{t} = \begin{cases} \eta^{+}\Delta_{ij}^{t-1}, & \text{if } \frac{\partial E^{t-1}}{\omega_{ij}} \frac{\partial E^{t}}{\omega_{ij}} > 0 \\ \eta^{-}\Delta_{ij}^{t-1}, & \text{if } \frac{\partial E^{t-1}}{\omega_{ij}} \frac{\partial E^{t}}{\omega_{ij}} < 0 \\ \Delta_{ij}^{t-1}, & \text{else} \end{cases} \qquad \text{(Eq. 3.8)}$$

If the error function has changed its sign this indicates the previous update was too large, thus the previous update is decreased by factor η^{-}. If the sign of the error function has not changed the update is increased by factor η^{+} in order to accelerate convergence. The direction of the update to the weight then is determined by the following:

$$\Delta w_{ij}^{t} = \begin{cases} -\Delta_{ij}^{t}, & \text{if } \frac{\partial E^{t}}{\omega_{ij}} > 0 \\ +\Delta_{ij}^{t}, & \text{if } \frac{\partial E^{t}}{\omega_{ij}} < 0 \\ 0, & \text{else} \end{cases} \qquad \text{(Eq. 3.9)}$$

$$w_{ij}^{t+1} = w_{ij}^{t} + \Delta\omega_{ij}^{t} \qquad \text{(Eq. 3.10)}$$

A positive derivative of the performance function E indicates an increase in error; therefore the update value is negative. Likewise a negative derivative corresponds to a decrease in error and the update value is added. One exception occurs in the case of a step being to large and the partial derivative changes signs. In this case a back tracking step is added:

$$\Delta\omega_{ij}^{t} = -\Delta\omega_{ij}^{t-1}, \text{ if } \frac{\partial E^{t-1}}{\omega_{ij}} \frac{\partial E^{t}}{\omega_{ij}} < 0 \qquad \text{(Eq. 3.11)}$$

Since the step after the back tracking step would create the same sign change in the partial derivative, no new update value is calculated and the previous update value (calculated during the back tracking step) is used.

In order to obtain the stable and fast performance of the algorithm, values of the initial update value (Δ^0), decrease factor (η^-), and increase factor (η^+) must be chosen. The initial update is not critical at all. In most cases the default value of $\Delta^0 = 0.1$ is expectable. Riedmiller and Braun found that constantly fixing the increase/decrease factors to $\eta^+ = 1.2$ and $\eta^- = 0.5$ works in most situations.

3.3 Alternative Networks

Up to this point, only multilayer feed-forward networks with sigmoid transfer functions have been considered. As problems get more complex,

larger networks are needed. Larger networks require the design to provide more parameters (number of layers, number of neurons per layer, transfer functions) to define the network and more computing power for adequate training. It becomes obvious that multilayer network design with back propagation training is unfeasible for some problems. One alternative to avoid these problems is the use of radial basis networks. The key feature of this type of network is the use of a radial basis function (Figure 3.5) in the hidden layer.

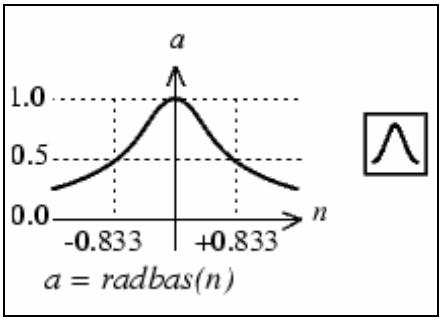

Figure 3.5: MATLAB Radial Basis Function

MATLAB defines the radial basis function as

$$a = e^{-n^2} \qquad \text{(Eq. 3.12)}$$

Although the network has weights and biases, they are used differently than in the case of the feed-forward network. The net input to the radial basis function is the Euclidean distance between its weight vector and the input vector, multiplied by the bias.

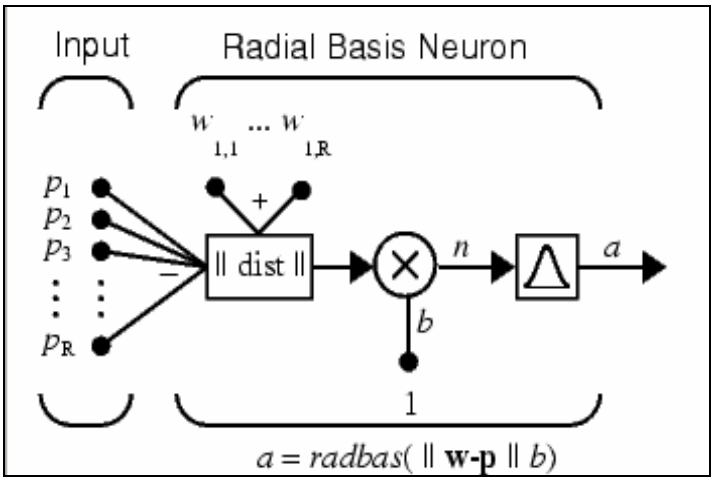

Figure 3.6: Radial Basis Neuron

The radial basis network does not require the designer to choose the size of the network; instead the training algorithm decides the network size in addition to the weights. The network begins as one hidden radial basis neuron and a layer of linear neurons equal in size to the output vector. At each iteration the input vector that results in a reducing the mean square error of the network the most is used to create a radial basis neuron and add it to the hidden layer. A new weight matrix for the linear output layer is created by dividing the output of the hidden layer by the desired output of the network. The error of the new network is calculated, and if it is less than or equal to the goal the training algorithm is finished. Otherwise another neuron is created. This process repeats until the goal is met or until the user specified number of hidden neurons is reached.

CHAPTER 4: APPROACH

4.1 System Overview

Input data is obtained from steering angle and accelerator pedal position via optical encoders. A pre-processing step, based on the hypothesis that jerk profiles are indicative of alertness level, differentiates the position data to find the jerk profile and calculates the associated parameter, spikiness index (see 4.2.2) (Desai and Haque, 2006). The output from the pre-processing is used as input to an artificial neural network. The neural networks used in this approach are inspired by Thompson et al. (2002) where the difference between the input and output of an artificial neural network autoencoder is used to detect abnormal system behavior. As opposed to other methods in the literature, which use classifier networks, this approach uses a special type of artificial neural network, referred to as an auto associative neural network. In auto associative neural networks the input is

equal to the target output during training. The advantage of using auto association is that only one type of input is needed to train the network, where a classifier network would require both drowsy and non-drowsy data sets. Since the network is trained to replicate its input as its output, data sets that are similar to training sets will pass through the network without being changed and data sets that differ from the training sets will be distorted. This change produced by the auto associative network is used to gauge how the test data set has changed from the training data sets. Thus, the inputs to the network are subtracted from the outputs and this difference is quantified by the sum squared error:

$$E = \sum_{i=1}^{n} \left(output_i - input_i \right)^2 \qquad \text{(Eq. 4.1)}$$

This approach is outlined in a flowchart, shown in Figure 4.1.

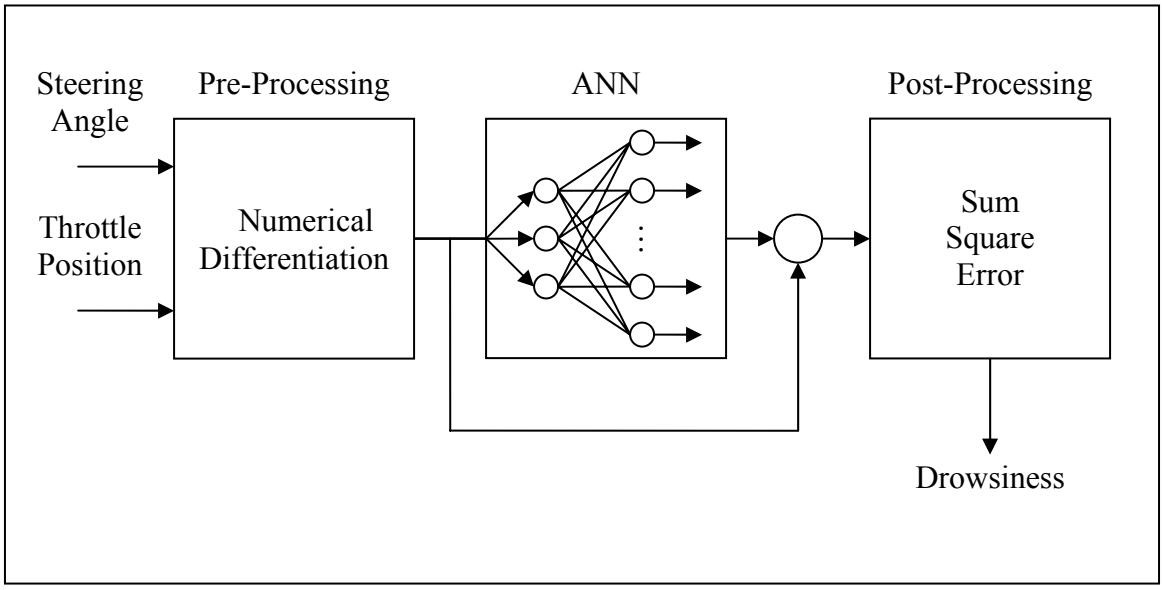

Figure 4.1: System Flow Chart

4.2 Input Processing

Instead of image processing or lane tracking techniques, both of which require extra sensors and real time image processing, this study introduces a method of monitoring driver drowsiness from the steering wheel and accelerator pedal. Steering angle and accelerator pedal position cannot alone measure drowsiness because they are significantly affected by traffic, landscape, etc., however, the time derivatives may be used to mask most of these variables. Because alert drivers respond quicker and more frequently than drowsy drivers, jerk profiles change as drivers become drowsy.

4.2.1 Savitzky-Golay Filter for Numerical Differentiation

The data for steering position and throttle are differentiated three times using the Savitzky-Golay method to give the velocity, acceleration and jerk. The Savitzky-Golay method finds filter coefficients b_n for a least squares fit polynomial within a moving window. In this case, a relatively small 7-point moving window is used to preserve most of the characteristics of the raw data. Since the third derivative of the data is needed, a cubic polynomial is used to fit the data in the form of

$$x = b_0 + b_1 t + b_2 t^2 + b_3 t^3 \qquad \text{(Eq. 4.2)}$$

The process of least squares fitting involves only a linear matrix inversion; the coefficients of the fitted polynomial are themselves linear. That means the fitting is done in advance, for fictitious data consisting of all zeros

except for a single one, and then the fit of the real data are linear combinations (Press 1992). Seven dummy variables are defined as

$$t_{i-3} = -3,\ t_{i-2} = -2,\ t_{i-1} = -1,\ t_i = 0,\ t_{i+1} = 1,\ t_{i+2} = 2,\ t_{i+3} = 3 \qquad \text{(Eq. 4.3)}$$

The method performs a least-squares fit of the cubic polynomial to all points in the moving window. Rearranging the equations for the polynomial with the dummy variables into matrix notation leaves

$$\begin{Bmatrix} x_{i+3} \\ x_{i+2} \\ x_{i+1} \\ x_i \\ x_{i-1} \\ x_{i-2} \\ x_{i-3} \end{Bmatrix} \approx \begin{bmatrix} 1 & 3 & 9 & 27 \\ 1 & 2 & 4 & 8 \\ 1 & 1 & 1 & 1 \\ 1 & 0 & 0 & 0 \\ 1 & -1 & 1 & -1 \\ 1 & -2 & 4 & -8 \\ 1 & -3 & 9 & -27 \end{bmatrix} \begin{Bmatrix} b_0 \\ b_1 \\ b_2 \\ b_3 \end{Bmatrix} \qquad \text{(Eq. 4.4)}$$

$$\{Y\} \approx [X]\{\beta\} \qquad \text{(Eq. 4.5)}$$

$$\{Y\} = \begin{Bmatrix} x_{i+3} \\ x_{i+2} \\ x_{i+1} \\ x_i \\ x_{i-1} \\ x_{i-2} \\ x_{i-3} \end{Bmatrix} \qquad \{\beta\} = \begin{Bmatrix} b_0 \\ b_1 \\ b_2 \\ b_3 \end{Bmatrix} \qquad \text{(Eq. 4.6, Eq. 4.7)}$$

$$[X]=\begin{bmatrix}1 & 3 & 9 & 27\\ 1 & 2 & 4 & 8\\ 1 & 1 & 1 & 1\\ 1 & 0 & 0 & 0\\ 1 & -1 & 1 & -1\\ 1 & -2 & 4 & -8\\ 1 & -3 & 9 & -27\end{bmatrix} \quad \text{(Eq. 4.8)}$$

Finally, the least squares solutions is

$$\{\beta\}=\left([X]^T[X]\right)^{-1}[X]^T$$

$$=\frac{1}{252}\begin{bmatrix}-24 & 36 & 72 & 84 & 72 & 36 & -24\\ -22 & 67 & 58 & 0 & -58 & -67 & 22\\ 15 & 0 & -9 & -12 & -9 & 0 & 15\\ 7 & -7 & -7 & 0 & 7 & 7 & -7\end{bmatrix}\begin{Bmatrix}x_{i+3}\\ x_{i+2}\\ x_{i+1}\\ x_i\\ x_{i-1}\\ x_{i-2}\\ x_{i-3}\end{Bmatrix} \quad \text{(Eq. 4.9)}$$

This polynomial is used only at point the x_i, a new polynomial is fit at the next point x_{i+1} using a shifted window. The least squares polynomial fit of the data is differentiated to find the jerk profile

$$x''' = \frac{6b_3\, t}{(\Delta t)^2} \quad \text{(Eq. 4.10)}$$

The equations for the smoothed data and first, second and third time derivatives are

$$x_i''' = \frac{x_{i+3} - x_{i+2} - x_{i+1} + x_{i-1} + x_{i-2} - x_{i-3}}{6\Delta t^3} \quad \text{(Eq. 4.11)}$$

Complete tables of the filter coefficients are available in Savitsky and Golay (1964).

This method creates a -3 dB low-pass cutoff at 16% of the sampling frequency. The main advantages of the Savitzky-Golay Method are that it tends to preserve features of the distribution such as relative maxima, minima and width. Also, when using this method to differentiate, it does not introduce distortions that are often associated with lower level finite difference methods. If the window for interpolation is small and if a high ordered polynomial is used very little alteration of the original data occurs. Figures 4.2 and 4.4 show the effects of the Savitzky-Golay filter on the raw data. The filter has altered the raw data very litte.

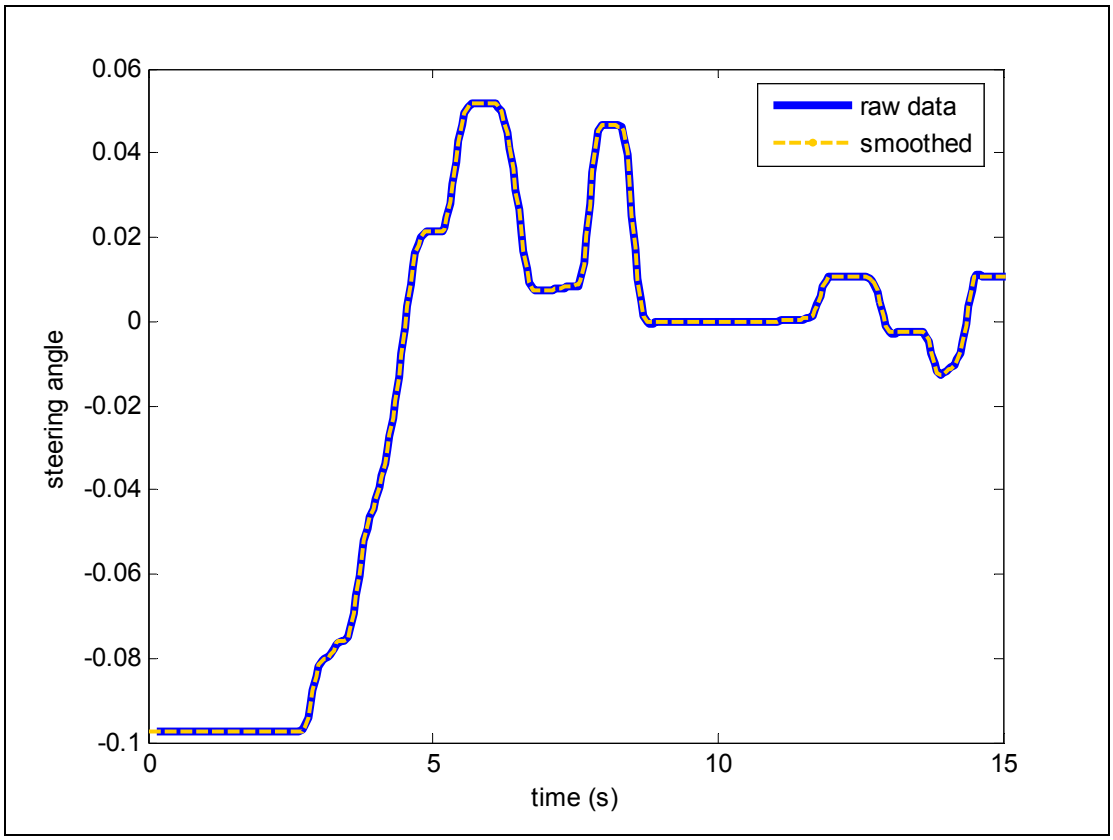

Figure 4.2: Raw and Smoothed Steering Position Data

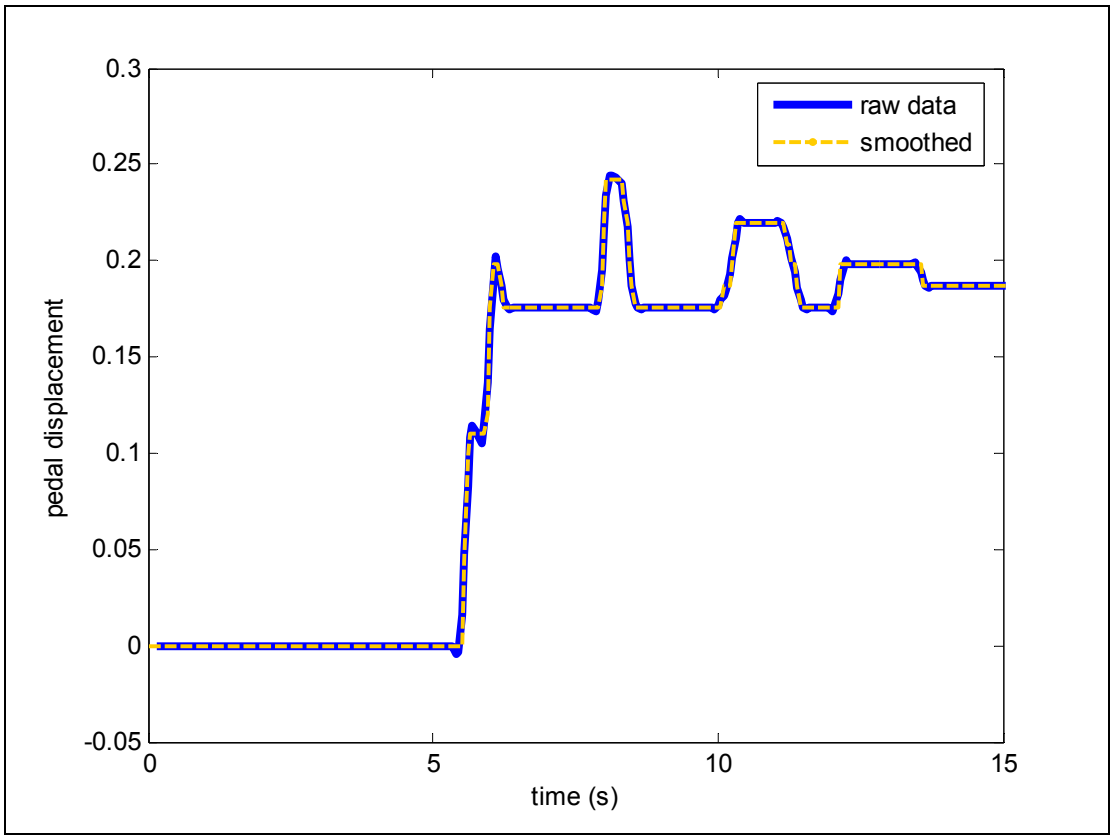

Figure 4.3: Raw and Smoothed Accelerator Pedal Position Data

4.2.2 Spikiness Index

The deviation of the jerk from the general trend of the data will also be used as an input for the neural network (Desai and Haque, 2006). To measure the deviation from the general trend, the spikiness index is used. To compute the spikiness index (Ψ) during 30 seconds of driving, the deviation from the general trend (μ_m) is calculated. The general trend (μ_m) is the average of a fixed number of points ($n_{avg} \leq n$) and is equivalent to a local average. Thus, for every point, the deviation from the general trend of the

points preceding it (specifically n_{avg} number of points) is computed to estimate the spikiness index. Figure 4.4 shows this definition graphically.

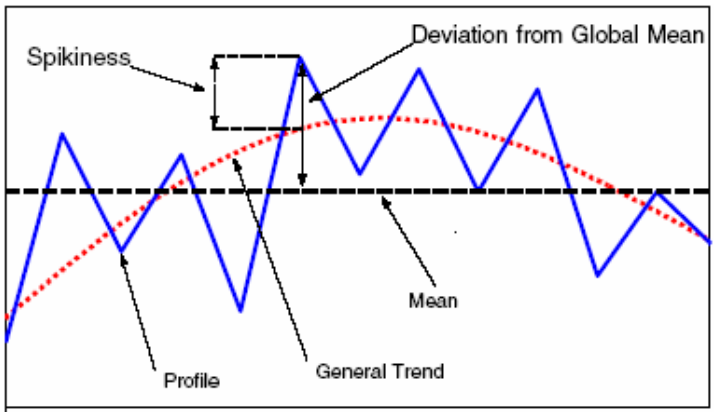

Figure 4.4: Definition of Spikiness (Desai and Haque, 2006)

The equation for spikiness index, according to the deviation from the general trend, is given by Desai and Haque (2006) as,

$$\Psi = \frac{\sum_{i=n_{avg}+1}^{n} \left(x_i - \frac{\sum_{j=i-n_{avg}}^{i-1} x_j}{n_{avg}} \right)^2}{n - n_{avg}} \qquad \text{(Eq. 4.12)}$$

It should be noted that n_{avg} determines the closeness of the plot to the actual profile; as n_{avg} increases the plot flattens out and eventually becomes a straight line (global mean of the data). For this analysis, n_{avg} is chosen to be 30 points (i.e. 1.5 seconds of drive time). The spikiness index of jerk of both steering angle and throttle is calculated for each 30-second interval of every driving run and recorded.

4.3 Artificial Neural Network Designs

Artificial neural networks are used to analyze the steering and accelerator pedal information. Two different neural network architectures are used for auto association (feed-forward and radial basis) each with two different input sets (jerk profile and spikiness index of jerk profile), for a total of four network designs. The first feed-forward network uses 2400 data points from the jerk profile of the steering and accelerator pedal for a single 4800 element input vector. The network consists of one hidden layer, containing 480 neurons, and an output layer of 4800 neurons. The second feed-forward network uses 20 spikiness indices from the jerk profiles of steering and accelerator pedal as a 40 element input vector. The spikiness index feed-forward network consists of one hidden layer, containing 480 neurons, and an output layer of 40 neurons. Tangent sigmoid transfer functions are used at the hidden layer and linear transfer functions are used at the output of both networks.

Like the feed-forward networks, the radial basis networks consist of one hidden layer and one output layer. The input and output layers of the two radial basis networks are identical to the corresponding feed-forward network—the jerk profile network has 4800 neurons in the output layer and a 4800 element input vector and the spikiness index network has 40 neurons in the output layer and a 40 element input vector.

4.4 Network Training

As previously mentioned, the only training sets required are data representing the driver's normal state. The first six simulation runs were used for the training sets. These sets were acquired between 6 pm and 12 am. Unfortunately, fewer data sets were collected for participant seven and participant eight. In order to keep the ratio of training sets to total data sets near 1:3.667 (like the other participants), five training sets were used for participant seven and four sets were used for participant eight.

The feed-forward networks were trained with the RPROP algorithm, a typical training record is shown in Figure 4.5.

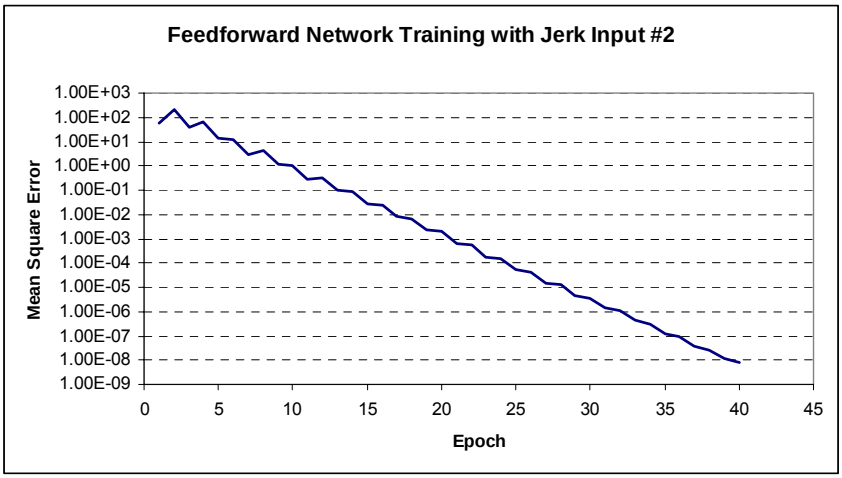

Figure 4.5: Example Training Record for Feedforward Network Using Jerk Profile

The training process was repeated using radial basis networks. As mentioned earlier, the radial basis network has a self-organizing layer. Initially the hidden layer has no neurons. Figures 4.6 through 4.8 show the training of the radial basis networks with jerk profile inputs.

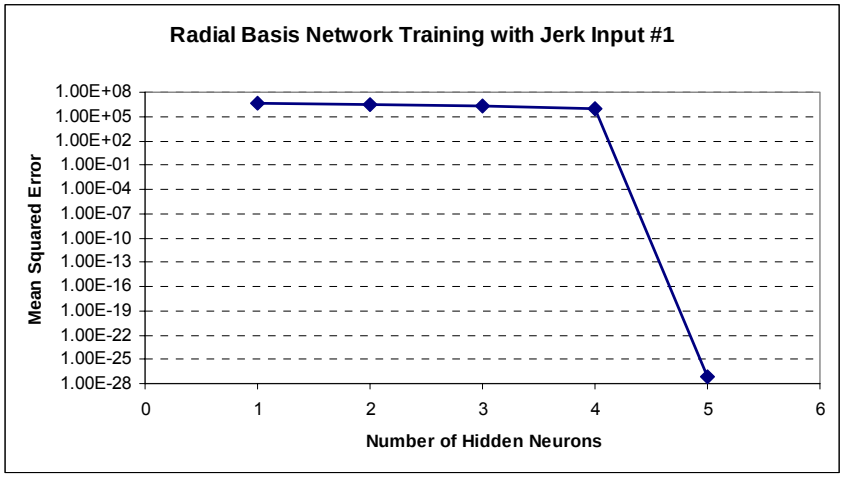

Figure 4.6: Example Training Record for Radial Basis Network Using Jerk Profile

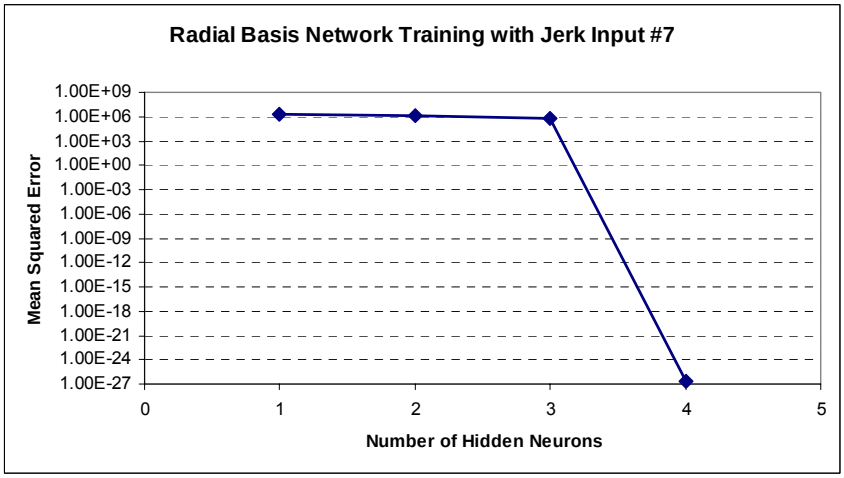

Figure 4.7: Training Record for Radial Basis Network Using Five Jerk Profiles

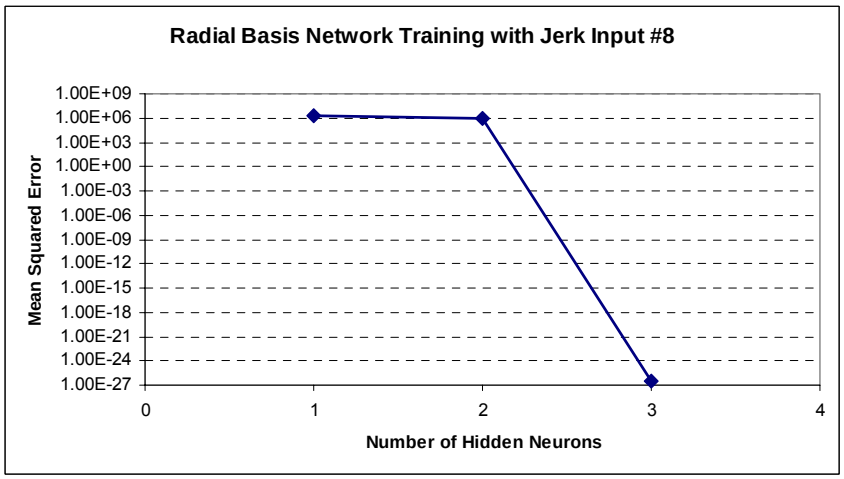

Figure 4.8: Training Record for Radial Basis Network Using Four Jerk Profiles

In an effort to compare the effects that the inputs to the artificial neural network have on the trends predicted by the drowsiness indicator, feed-forward and radial basis networks were trained with the same training sets, algorithms, and training goals using spikiness index inputs. Some feedforward networks did not reach the desired mean square error (Figure 4.10 and 4.11). The radial basis networks trained very similiarly to the jerk profile networks.

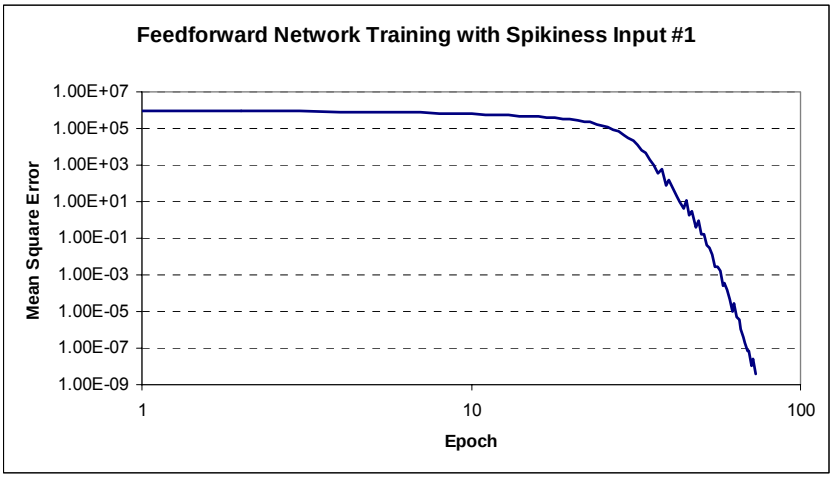

Figure 4.9: Training Record for Feedforward Network Using Spikiness Index

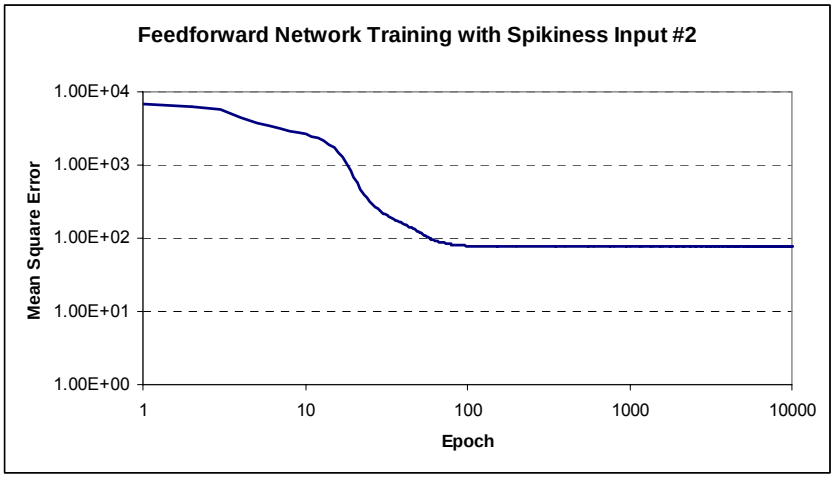

Figure 4.10: Training Record for Network Trapped in Local Minima

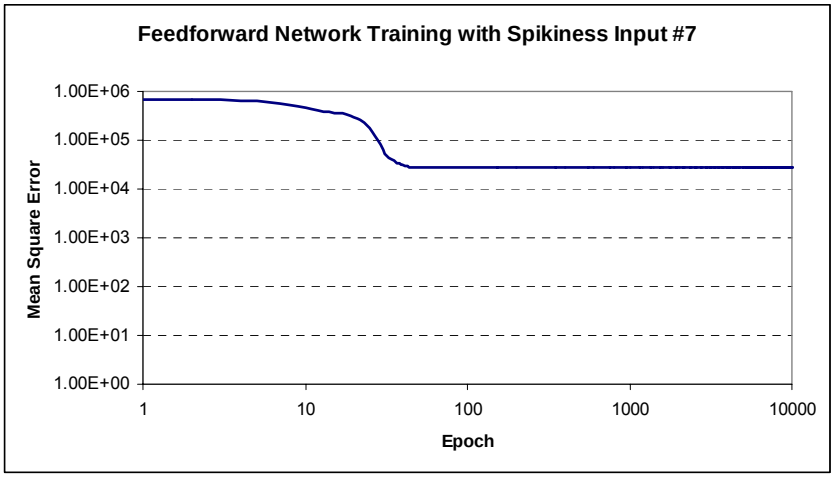

Figure 4.11: Training Record for Network Trapped in Local Minima

CHAPTER 5: RESULTS

5.1 Jerk Profiles

Once the artificial neural networks described in Chapter 4 were trained using the data sets obtained from the experiment described in Chapter 2, the networks were tested using the remaining data sets. The drowsiness indicator number

$$E = \sum_{i=1}^{n} \left(output_i - input_i \right)^2 \qquad \text{(Eq. 5.1)}$$

was normalized by dividing all of the indicator numbers by the maximum indicator number. The indicator numbers were arranged from the earliest test (roughly 12 AM) to the latest (roughly 6 PM) and a linear trend line was added to the plot. Figures 5.1 through 5.8 show the drowsiness indicator results using the jerk profiles of steering and accelerator pedal as inputs to feed-forward and radial basis networks.

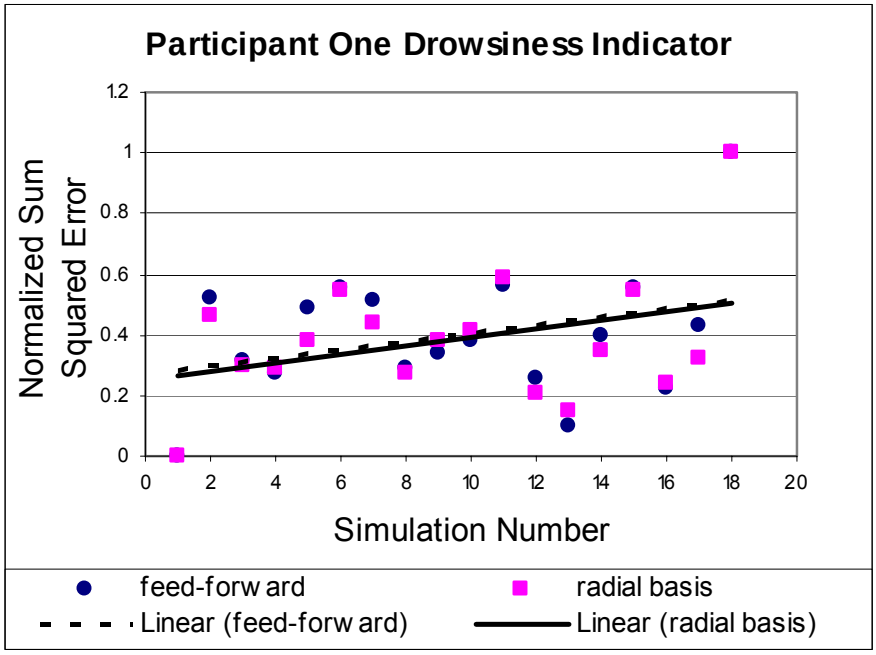

Figure 5.1: Drowsiness Indicator using Jerk Profile #1

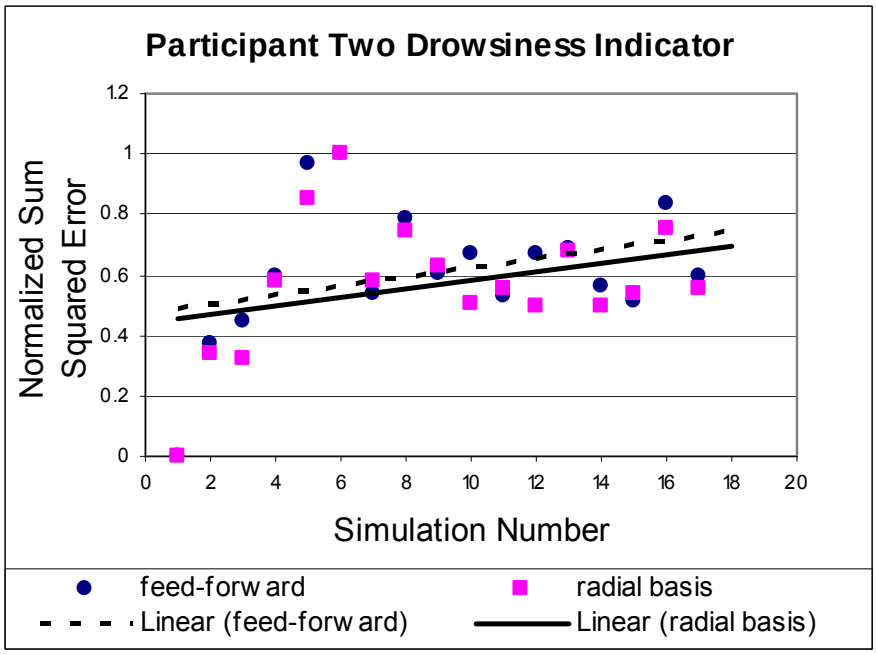

Figure 5.2: Drowsiness Indicator using Jerk Profile #2

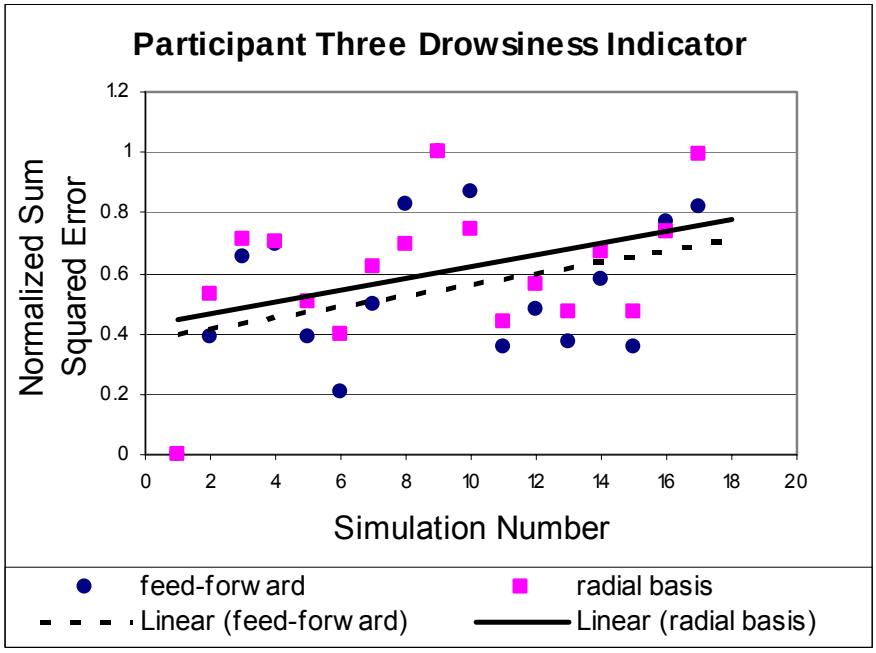

Figure 5.3: Drowsiness Indicator using Jerk Profile #3

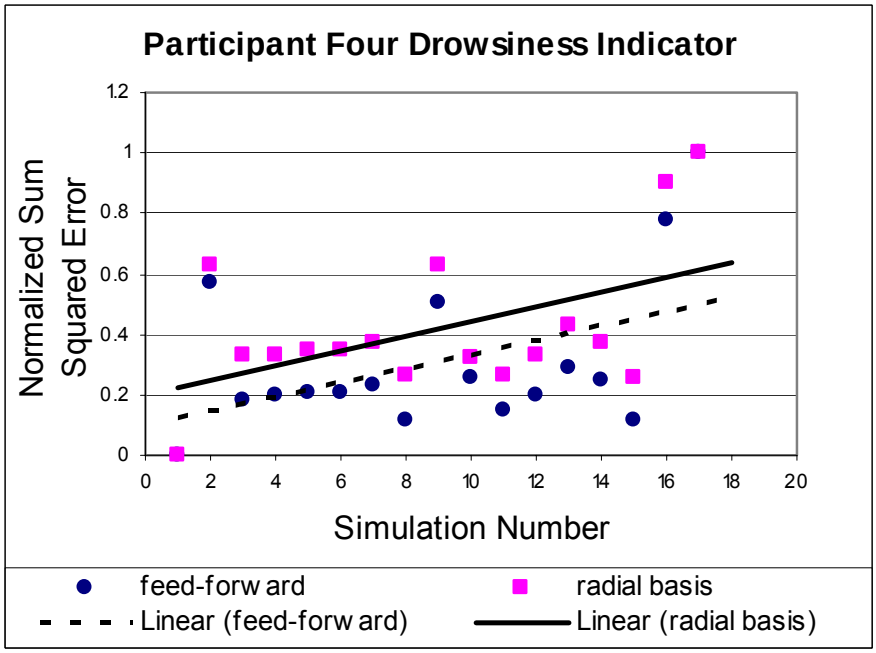

Figure 5.4: Drowsiness Indicator using Jerk Profile #4

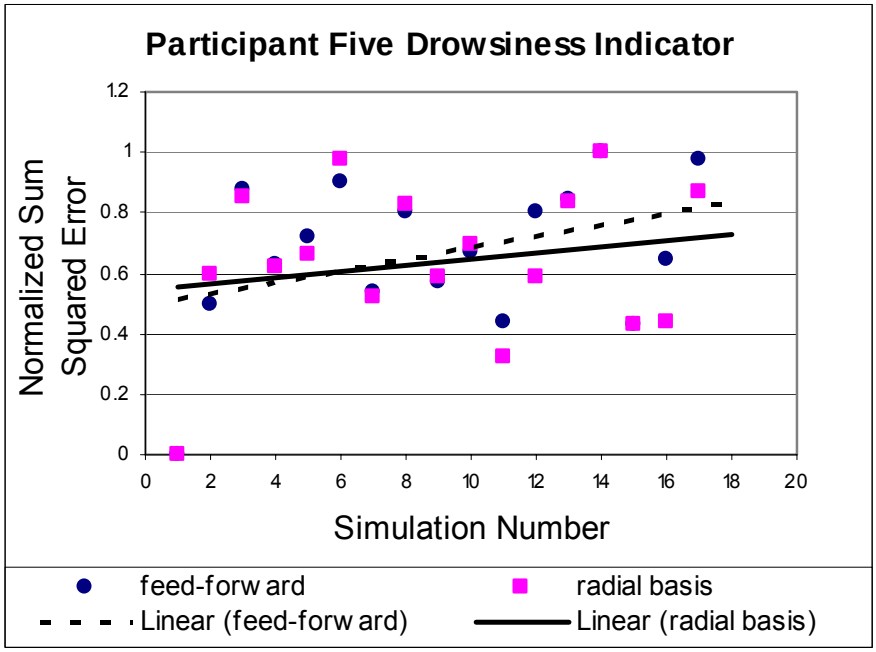

Figure 5.5: Drowsiness Indicator using Jerk Profile #5

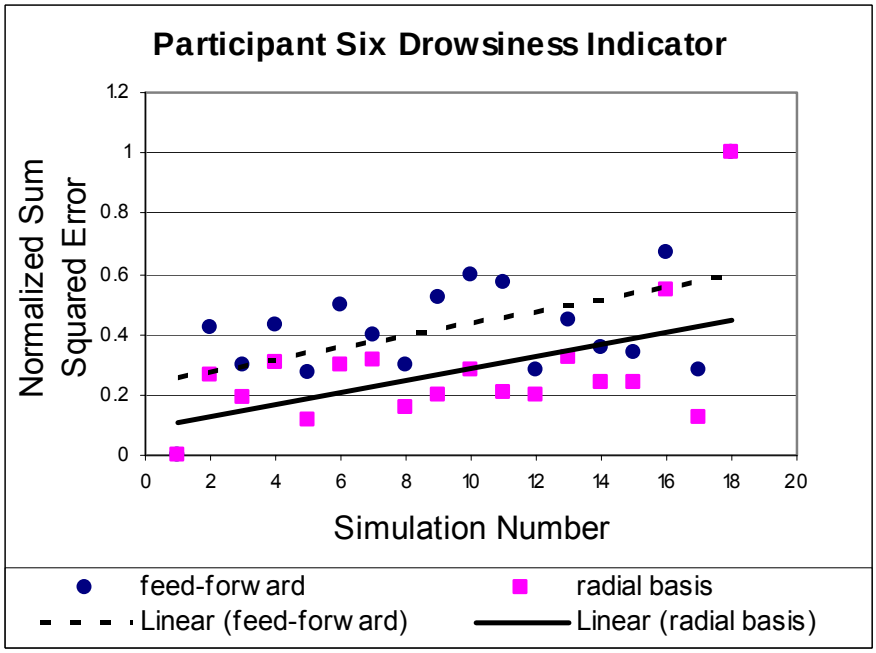

Figure 5.6: Drowsiness Indicator using Jerk Profile #6

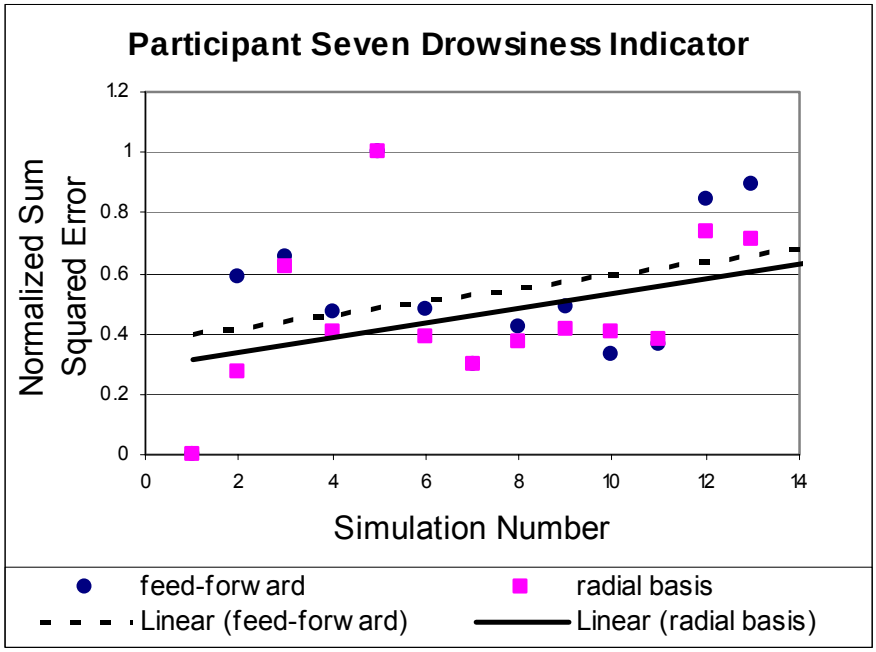

Figure 5.7: Drowsiness Indicator using Jerk Profile #7

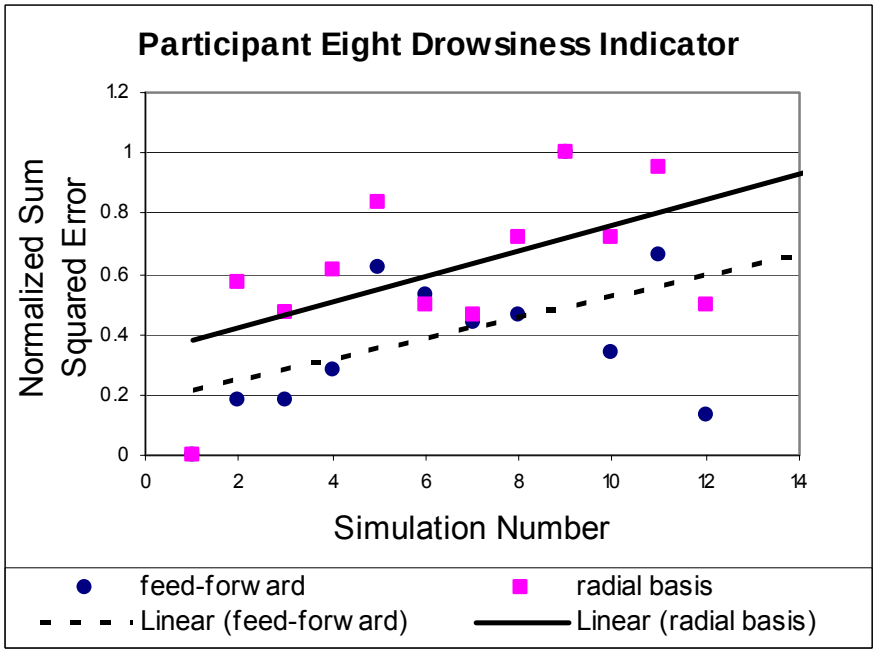

Figure 5.8: Drowsiness Indicator using Jerk Profile #8

When using the jerk profile as the input, all of the participants showed a positive trend, indicating that the driver's steering and accelerator pedal jerk profiles strayed further from the sets used for training the longer the

participant stayed awake. These trends are justified by the work of Dinges, et al. (2001) which shows the longer a person stays awake past 18 hours, the further their performance will decrease. Interestingly several participants showed higher error levels near dawn (most notably Figures 5.2, 5.5, 5.7, and 5.8) and in the late afternoon (most notably Figures 5.1, 5.3, 5.4, and 5.7). These phenomena are explained by a study by Sagberg, et al. (2004), which shows people who have been asked to stay awake for 24 continuous hours will have unintended sleep episodes, most often around 6 am and in the middle of the afternoon, caused by the circadian rhythm. Using a radial basis neural network instead of a feed-forward neural network introduces a bias, but does not significantly alter the trend of the drowsiness indicator.

5.2 Spikiness Index

In an effort to compare the effects that the inputs to the artificial neural network have on the trends predicted by the drowsiness indicator, feed-forward and radial basis networks were tested using the spikiness index inputs as described in Chapter 4. Figures 5.9 through 5.16 show the drowsiness indicator results using spikiness indices as inputs to feed-forward and radial basis networks.

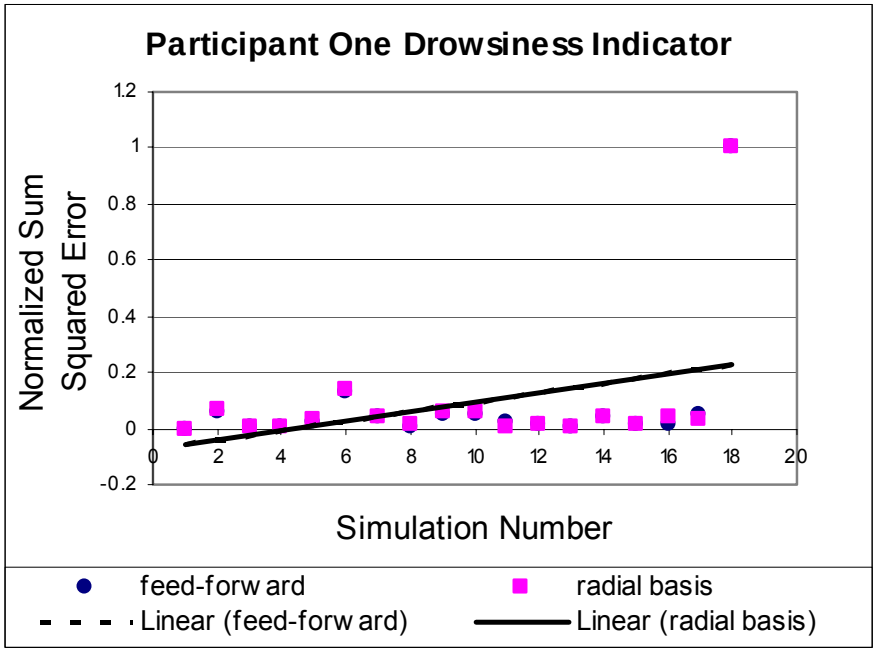

Figure 5.9: Drowsiness Indicator using Spikiness Index #1

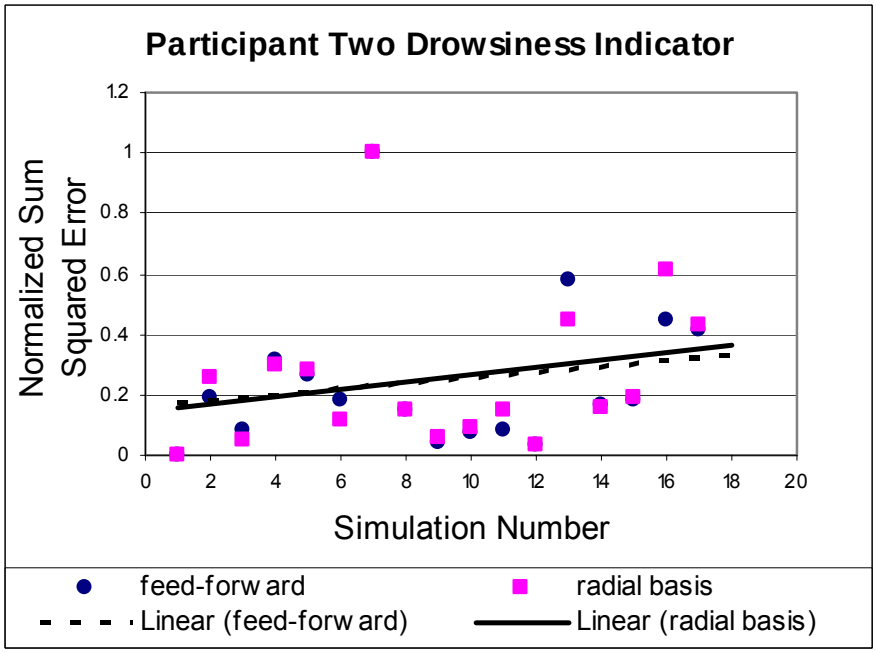

Figure 5.10: Drowsiness Indicator using Spikiness Index #2

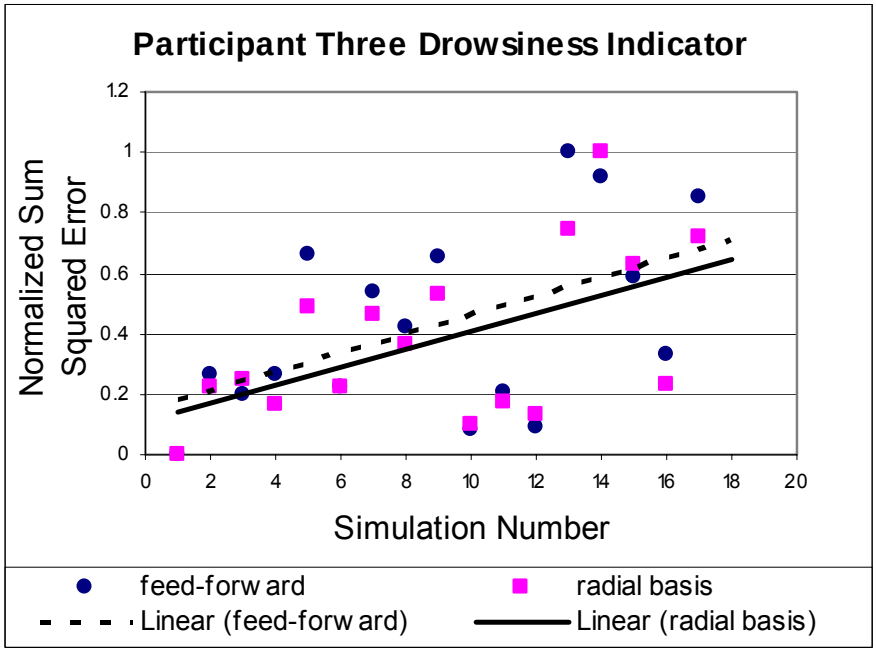

Figure 5.11: Drowsiness Indicator using Spikiness Index #3

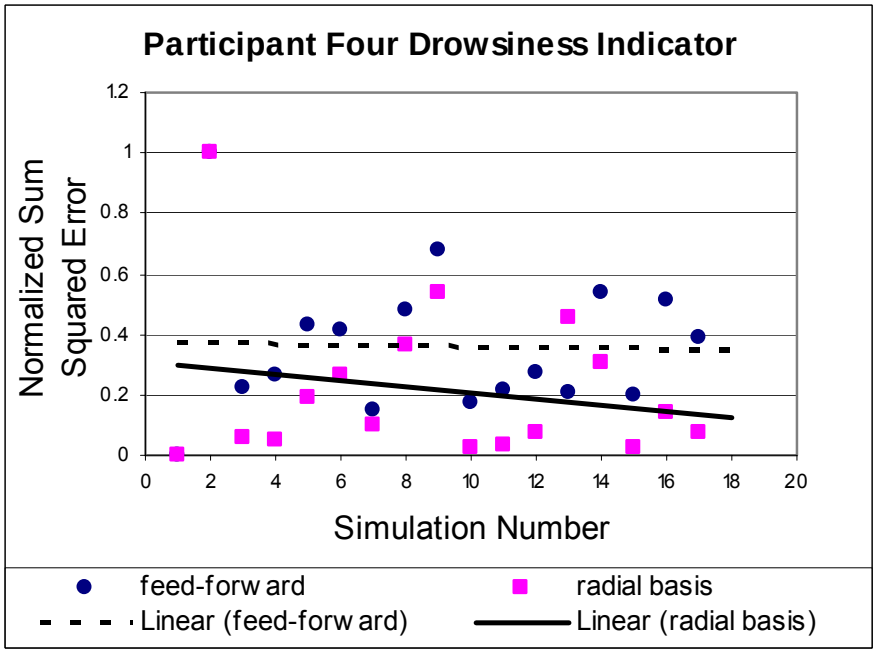

Figure 5.12: Drowsiness Indicator using Spikiness Index #4

Participant four (Figure 5.12) changed dramatically when spikiness index was used. The maximum difference from the training set is predicted at a very different, and unexpected, time and the trend line has reversed in direction.

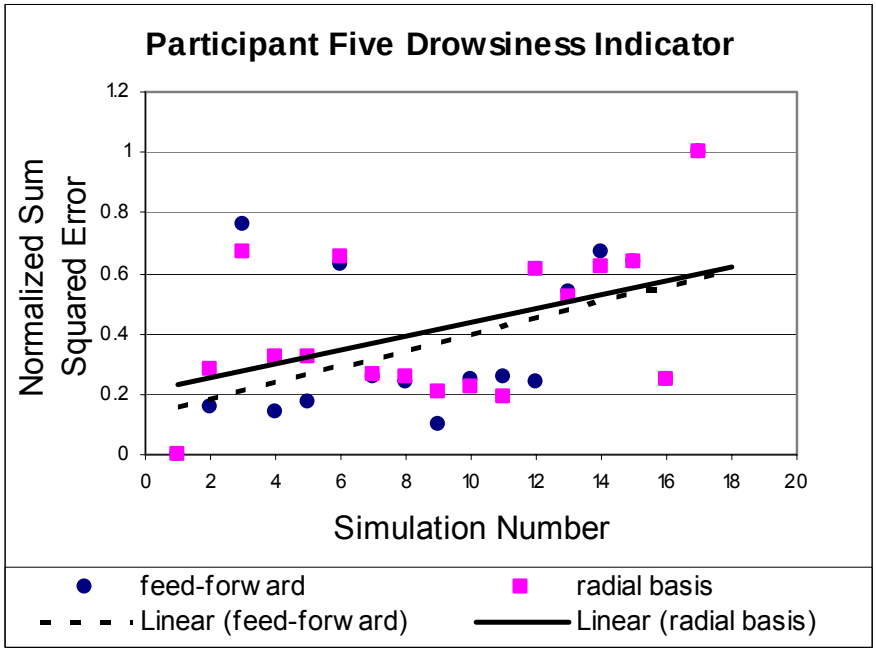

Figure 5.13: Drowsiness Indicator using Spikiness Index #5

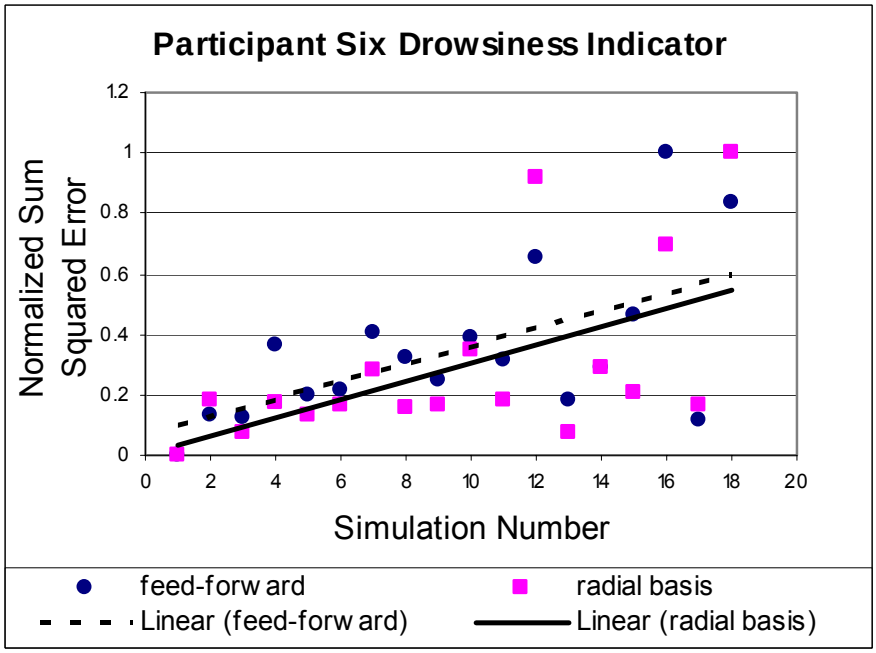

Figure 5.14: Drowsiness Indicator using Spikiness Index #6

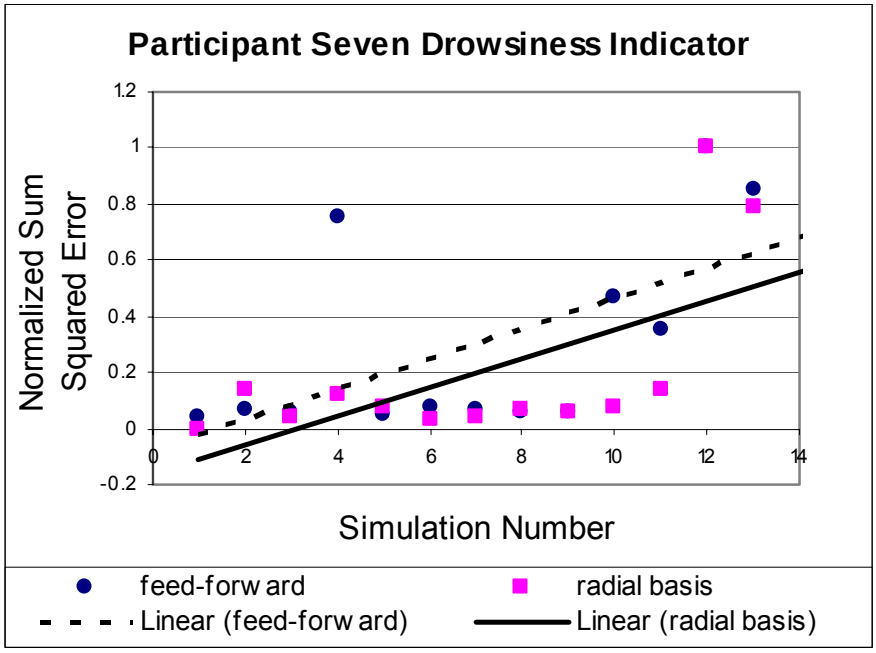

Figure 5.15: Drowsiness Indicator using Spikiness Index #7

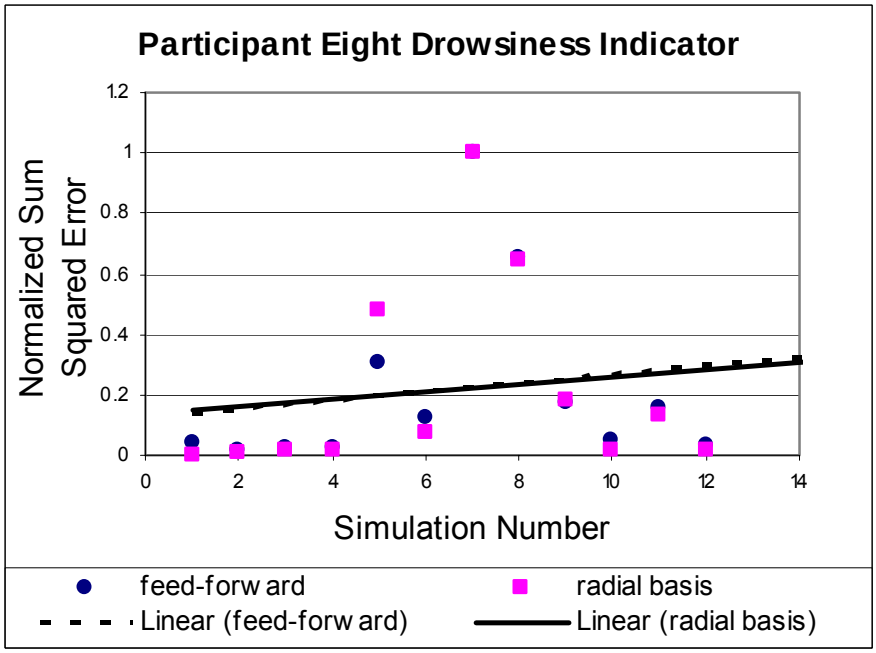

Figure 5.16: Drowsiness Indicator using Spikiness Index #8

The networks with spikiness indices as inputs had different outputs than the networks using jerk profile, but most drowsiness indicator trends were similar. The networks predicted maximum difference from the training sets at

similar times for most participants. The radial basis network and feed-forward network produced trends in the drowsiness indicator that are extremely similar for participants one, two and eight (Figure 5.9, Figure 5.10, and Figure 5.16) or introduced a very small bias (Figure 5.11, Figure 5.14, and Figure 5.15).

CHAPTER 6: Conclusion

Artificial neural networks using jerk profiles as inputs predicted drowsiness indicators that matched expectations from the literature. Changing the network architecture did not provide better results, but the combination of self-organization and supervised learning used by the radial basis network is significantly faster than the back-propagation training used by the feed-forward network. Also, the hidden layer of the radial basis network contains 5 neurons. Compared to the 480 used in the feed-forward design, this is quite a reduction in network size, and as a result, a reduction in computer storage required to implement the network.

Although the results of one of the participants reduced in quality, the spikiness index can still be a useful parameter for drowsiness prediction. The spikiness index as implemented reduces the number of inputs to the network because it effectively compresses 20 seconds of jerk profile (400 data points) into one data point, this leads to a smaller number of inputs and a smaller

network. Further work should include a redesign of the spikiness index inputs. The number of data points used to calculate the spikiness index (n) and the number of data points used for local averaging (n_{AVG}) can be changed, possibly creating favorable changes in network performance.

Since the data used to test the system design was obtained from simulated driving, real life driving is needed to verify the system. Simulated driving is convenient because of the safety for the driver, but it cannot produce the sensation of road vibration, wind or the element of danger from real-life driving.

References

Allen, R. W., Rosenthal, T. J., and Szostak, H. T. (1988) “Analytical Modeling of Driver Response in Crash Avoidance Maneuvering – Volume II: An Interactive Tire Model,” NHTSA Final Report DOT-HS-807-271

Allen, R. W., Rosenthal, T. J., and Szostak, H. T. (1988) “Analytical Modeling of Driver Response in Crash Avoidance Maneuvering – Volume III: A Trim Model and Computer Program for Determining Ground Vehicle Steady State Operating Conditions and Quasilinear Stability Coefficients,” NHTSA Final Report DOT-HS-807-272

Allen, R. W., Rosenthal, T. J., and Szostak, H. T. (1988) “Analytical Modeling of Driver Response in Crash Avoidance Maneuvering – Volume IV: User’s Guide for Linear Analysis, Nonlinear Simulation, Part Task Simulation,” NHTSA Final Report DOT-HS-807-273

Andreeya, E., Aarabi, P., Philiastides, M. G., Mohajer, K. and Emami, M., (2004) “Driver Drowsiness Detection Using Multi-Modal Sensor Fusion,” Proceedings of SPIE - Multisensor, Multisource Information Fusion: Architectures, Algorithms, and Applications, 5434, pp. 380-390

Aserinsky, E. and Kleitman, N. (1953) “Regularly Occurring Periods of Eye Motility, and Concomitant Phenomena during Sleep,” Science, 118(3062), pp. 273-274

AssistWare Technology. Available: http://www.assistware.com

Attention Technologies, Inc. (2005) Available: http://www.attentiontechnology.com/index.html

Bekiaris, E., Nikolaou, S., and Mousadakou A., (2004) “AWAKE: Design Guidelines for Driver Drowsiness Detection and Avoidance,” Hellenic Institute of Transport, Thessaloniki, Greece

Bergasa, L. M., Nuevo, J., Sotelo, M. A., and Vazquez, M., (2004) “Real-Time System for Monitoring Driver Vigilance,” 2004 IEEE Intelligent Vehicles Symposium, 14-17 June, pp. 78-83

Brandt, T., Stemmer, R., and Rakotonirainy, A., (2004) "Affordable visual driver monitoring system for fatigue and monotony," 2004 IEEE International Conference on Systems, Man and Cybernetics, 10-13 Oct, 7, pp. 6451- 6456

Carpenter, G. A., (1989) Neural Network Models for Pattern Recognition and Associative Memory,” Neural Networks, 2(4), pp. 243-257

Carpenter, G.A. and Grossberg, S., (1987) “A Massively Parallel Architecture for a Self-Organizing Neural Pattern Recognition Machine,” Computer Vision, Graphics, and Image Processing, 37, pp. 54–115

Carswell, B. and Chandran, V., (1994) “Automated recognition of drunk driving on highways from video sequences,” 1994 IEEE International Conference on Image Processing, 13-16 Nov, 2, pp. 306–310

Chang, J.Y., Cho, C.W., and Lu, S.M. (2005) “A Fuzzy Intergral Based Information Fusion for Drowsiness Detection,” International Journal of Fuzzy Systems, 7(2), pp.63-71

Chen, C.H., (1990) “On the Relationships between Statistical Pattern Recognition and Artificial Neural Networks,” 1990 IEEE International Conference on Systems, Man and Cybernetics, 4-7 Nov, pp.182 – 183

Chieh, T.C., Mustafa, M.M., Hussain, A., Zahedi, E., and Majlis, B.Y., (2003) “Driver Fatigue Detection Using Steering Grip Force,” 2003 Student Conference on Research and Development, 25-26 Aug, pp. 45–48

Chrstos, J. P., and Heydinger, G. J. (1997) “Evaluation of VDANL and VDM RoAD for Predicting the Vehicle Dynamics of a 1994 Ford Taurus,” SAE Paper No. 970566

Dawson, D., Feyer, A. M., Gander, P., Hartley, L., Haworth, N., Willamson, A., Baas, P., Nolan, D., Moore, B., Brooks, C., Foley, C. and Bottomley, B., (2001) “Fatigue Expert Group: Options for a Regulatory Approach to Fatigue in Drivers of Heavy Vehicles in Australia and New Zealand,” National Transport Commission Australia, Melbourne, Australia

Delahaye, N., and Kemeny, A., (1999) “PSU Truck Driving Simulator,” International Journal of Heavy Vehicle Systems, 6, pp. 391–397

Dement, W. and Kleitman, N., (1957) “The Relation of Eye Movements During Sleep to Dream Activity: An Objective Method for the Study of Dreaming,” Journal of Experimental Psychology, 53, pp. 339-346

Desai, A. V., and Haque, M. A., (2006) “Vigilance Monitoring for Operator Safety: A Simulation Study on Highway Driving,” Journal of Safety Research, 37, pp. 139-147

Desmond, P. A., and Hancock, P. A., (2001) *Stress, workload, and fatigue*, New Jersey, Lawrence Erlbaum Associates, pp. 455-465

Dinges, D. and Grace, R., (1998) “PERCLOS: a valid psychophysiologial measure of alertness as assessed by psychomotor vigilance,” Federal Highway Administration, Office of Motor Carriers, USA

Dinges, D., (1995) “An Overview of Sleepiness and Accidents,” Journal of Sleep Research, 4(2), pp. 4 – 14

Dinges, D., Maislin, G., and Van Dongen, H., (2001) “Chronic Sleep Restriction: Relation of Sleep Structure to Daytime Sleepiness and Performance,” Sleep, 24, A28

Eriksson, M. and Papanikolopoulos, N. P., (2001) “Driver fatigue: a Vision-Based Approach to Automatic Diagnosis,” Transportation research, Part C: Emerging technologies, 9(6), pp. 399-413

Faber, J., (2004) “Detection of Different Levels of Vigilance by EEG Pseudo Spectra,” Neural Network World, 14(3-4), pp. 285-290

Faber, J., Novak, M., Svoboda, P., and Tatarinov V., (2003) "Electrical Brain Wave Analysis During Hypnagogium," Neural Network World, 1, pp. 41-54

Fukuda, J., Akutsu, E., and Aoki K., (1995) "Estimation of driver's drowsiness level using interval of steering adjustment for lane keeping," JSAE Review, 16, pp. 197-199

Grace, R., Byrne, V.E., Bierman, D.M., Legrand, J. M., Gricourt, D., Davis, B.K., Staszewski, J.J. and Carnahan, B., (1998) “A Drowsy Driver Detection System for Heavy Vehicles,” 1998 AIAA/IEEE/SAE Digital Avionics Systems Conference, 31 Oct-7 Nov, 2, pp. I36/1 - I36/8

Hayashi, K.; Ishihara, K.; Hashimoto, H.; Oguri, K., (2005) “Individualized Drowsiness Detection during Driving by Pulse Wave Analysis with Neural Network,” 2005 IEEE Conference on Intelligent Transportation Systems, 13-15 Sept, pp. 901 – 906

Heydinger, G. J., Garrott, W.R., Chrstos, J. P., and Guenther, D.A. (1990) “A Methodology for Validating Vehicle Dynamics Simulations,” SAE Paper No. 900128

Hoskins, A. H., (2002) “Development and Validation of the Pennsylvania Truck Driving Simulator,” Masters Thesis, The Pennsylvania State University, University Park, Pa

Ji, Q., Zhu, Z., and Lan P., (2004) “Real-Time Nonintrusive Monitoring and Prediction of Driver Fatigue,” IEEE Transactions on Vehicular Technology, 53(4), pp.1052-1068

Jung, C. and Kelber, C., (2005) “A Lane Departure Warning System Using Lateral Offset with Uncalibrated Camera,” 2005 IEEE Conference on Intelligent Transportation Systems, 13-15 Sept, pp.348-353

Kaneda, M., Obara, H., and Nasu T., (1999) "Adaptability to ambient light changes for drowsy driving detection using image processing," JSAE Review, 20, pp. 133-136.

Kohonen, T., Barna, G. and Chrisley, R., (1988) “Statistical Pattern Recognition with Neural Networks: Benchmarking Studies,” 1988 IEEE International Conference on Neural Networks, 24-27 July, 1, pp. 61-68.

LeBlanc, D. J., Johnson, G. E., Venhovens, P. J. T., Gerber, G., DeSonia, R., Ervin, R. D., Lin, C.F., Ulsoy, A. G., and Pilutti, T. E., (1996) "CAPC: an implementation of a road-departure warning system," 1996 IEEE International Conference on Control Applications, 15-18 Sept, pp. 590-595

Makeig, S., Jung, T. P., and Sejnowski, T. J., (2000) “Awareness During Drowsiness: Dynamics and Electrophysiological Correlates,” Canadian Journal of Experimental Psychology, 54(4), pp. 266-273

McCulloch, W. S. and Pitts, W. H. (1943) “A Logical Calculus of the Ideas Immanent in Nervous Activity,” Bulletin of Mathematical Biophysics, 5, pp.115-133
Merriam Webster Dictionary [Online]

Nakano, T., Sugiyama, K., Mizuno, M. and Yamamoto, S., (1996) "Blink measurement by image processing and application to detection of driver's drowsiness," Terebijon Gakkaishi/Journal of the Institute of Television Engineers of Japan, 50, pp. 1949-1956

Press, W. H.; Flannery, B. P.; Teukolsky, S. A.; and Vetterling, W. T. (1992) *Numerical Recipes in FORTRAN: The Art of Scientific Computing*, Cambridge, England: Cambridge University Press, 2, pp. 183 and 644-645

Rau, P. S., (1996) “NHTSA’s Drowsy Driver Research Program Fact Sheet,” National Highway Traffic Safety Administration, Washington, DC

Riedmiller, M. and Braun, H. (1993) “A Direct Adaptive Method for Faster Backpropagation Learning: the RPROP Algorithm,” 1993 IEEE Internation Conference on Neural Networks, 28 Mar – 1 Apr, 1, pp. 586-591

Sagberg, F. Jackson, P., Krüger, H. P., Muzet, A., Williams, A., (2004) “Fatigue, Sleepiness and Reduced Alertness as Risk Factors in Driving,” Institute of Transport Economics, Oslo, Norway

Savitzky, A. and Golay, M. J. E. (1964) “Smoothing and Differentiation of Data by Simplified Least Squares Procedures,” Analytical Chemistry, 36, pp. 1627-1639

Sayed, R. and Eskandarian, A., (2001) "Unobtrusive drowsiness detection by neural network learning of driver steering," Proceedings of the Institution of Mechanical Engineers, Part D: Journal of Automobile Engineering, 215, pp. 969-975

Shor, R.E. and Thackray, R.I., (1970) “A Program of Research in Highway Hypnosis: A Preliminary Report,” Accident Analysis Prevention, 2(2), pp. 103-109

Smith, P., Shah, M., da Vitoria Lobo, N., (2000) “Monitoring Head/Eye Motion for Driver Alertness with One Camera,” 2000 International Conference on Pattern Recognition, 3-7 Sept, 4, pp. 636 – 642

Strohl, K. P., Blatt, J., Council, F., Georges, K., Kiley, J., Kurrus, R., McCartt, A. T., Merritt, S. L., Pack, A. I., Rogus, S., Roth, T., Stutts, J., Waller, P, and Willis, D., (1998) “Drowsy Driving and Automobile Crashes,” National Highway Traffic Safety Administration, Washington, DC

Stutts, J. C., Wilkins, J. W., and Vaughn, B. V., (1999) “Why Do People Have Drowsy Crashes: Input from Drivers Who Just Did,” AAA Foundation for Traffic Safety, Washington, DC

Tack, D. and Craw, I., (1996) “Tracking and Measuring Drivers’ Eyes” Image and Vision Computing, 14, pp. 541-547

Thiffault, P., and Bergeron, J., (2003) “Monotony of Road Environment and Driver Fatigue: A Simulator Study,” Accident Analysis and Prevention, 35(3), pp.381– 391

Thompson, B.B. Marks, R.J., II Choi, J.J. El-Sharkawi, M.A. Ming-Yuh Huang Bunje, C. (2002) “Implicit Learning in Autoencoder Novelty Assessment,” 3, pp. 2878-2883

Ueno, H., Kaneda, M. and Tsukino, M., (1994) “Development of Drowsiness Detection System,” 1994 IEEE Conference on Vehicle Navigation and Information Systems, 31 Aug-2 Sept, pp. 15-20

Vuckovic, A., Radivojevic, V., Chen, A. C. N., and Popovic, D., (2002) “Automatic Recognition of Alertness and Drowsiness from EEG by an Artificial Neural Network,” Medical Engineering and Physics, 24(5), pp. 349-360

Wang, J. S., Knipling, R. R., and Blincco, L. J., (1996) “Motor Vehicle Crash Involvements: A Multi-Dimensional Problem Size Assessments,” Paper presented at ITS 6th Annual Meeting, Houston, TX

Wierwille, W.W., Ellsworth, L.A., Wreggit, S.S., Fairbanks, R.J., and Kirn, C.L. (1994) “Research on vehicle based driver status/performance monitoring: development, validation, and refinement of algorithms for detection of driver drowsiness,” National Highway Traffic Safety Administration, Washington, DC

Wilson, B.J. and Bracewell, T.D., (2000) “Alertness Monitor Using Neural Networks for EEG Analysis,” 2000 IEEE Workshop on Neural Networks for Signal Processing, 11-13 Dec, 2, pp. 814–820

Yasui, N., Iisaka, A., and Nomura, N., (1998) "White Road Line Recognition Using Lane Region Extraction and Line Edge Detection," 1998 SAE International Congress and Exposition, 23-26 Feb, pp. 131-136